



## Late Neogene environmental changes in the central Himalaya related to tectonic uplift and orbital forcing

Yang Wang<sup>a,\*</sup>, Tao Deng<sup>b</sup>, Lawrence Flynn<sup>c</sup>, Xiaoming Wang<sup>d</sup>, An Yin<sup>e</sup>, Yingfeng Xu<sup>a</sup>, William Parker<sup>a</sup>, Eric Lochner<sup>f</sup>, Chunfu Zhang<sup>a</sup>, Dana Biasatti<sup>a,g</sup>

<sup>a</sup> Department of Earth, Ocean and Atmospheric Science, Florida State University and National High Magnetic Field Laboratory, Tallahassee, FL 32306-4100, USA

<sup>b</sup> Key Laboratory of Evolutionary Systematics of Vertebrates, Institute of Vertebrate Paleontology and Paleoanthropology, Chinese Academy of Sciences, Beijing 100044, China

<sup>c</sup> Peabody Museum, Harvard University, Cambridge, MA 02138, USA

<sup>d</sup> Department of Vertebrate Paleontology, Natural History Museum of Los Angeles County, 900 Exposition Boulevard, Los Angeles, CA 9007, USA

<sup>e</sup> Department of Earth and Space Sciences and Institute of Geophysics and Planetary Physics, University of California, Los Angeles, CA 90095-1567, USA

<sup>f</sup> Analytical Facilities, MARTECH, Tallahassee, FL 32306-4351, USA

<sup>g</sup> Two Medicine Dino Center, Bynum, MT 59419, USA

### ARTICLE INFO

#### Article history:

Available online 17 June 2011

#### Keywords:

Paleo-lake basin  
Mammalian fossils  
Stable isotopes  
Neogene environmental change  
Himalaya  
Tibetan Plateau

### ABSTRACT

The linkage between tectonic forces and climate evolution remains a matter of much debate and speculation. Here we present high-resolution oxygen and carbon isotope data from an ancient lake basin in the central Himalaya. These data, together with sedimentologic evidence, reveal major changes in drainage systems and depositional settings at  $\sim 7.2$ ,  $\sim 5.5$  and  $\sim 3.2$  Ma. These environmental changes appear to be driven by regional-scale tectonics. The oxygen isotope record also reveals alternating wet and dry climates with periodicities of 24 and 100 kyr that were likely controlled by orbital forcing. Paleo-temperatures, estimated using a fossil-based oxygen isotope “paleo-thermometer”, are  $21 \pm 6$  °C at  $\sim 7$  Ma, which is  $\sim 19 \pm 6$  °C higher than the present-day mean annual temperature in the same area. The much warmer environment inferred here is consistent with fossil mammalian and pollen assemblages and sediment clay mineralogy as well as carbon isotope data from fossil tooth enamels and paleosol carbonates. The estimated temperature difference would require the study area to have been raised by  $\sim 2$ – $2.5$  km since  $\sim 7$  Ma to its current elevation of 4100–4500 m above sea level. This result can be interpreted as either indicating the presence of a low-altitude intermountain basin in the hanging wall of the already formed Main Central Thrust or a protracted development of a north-trending rift basin that has experienced changes in drainage system and depositional environment through time.

© 2011 Elsevier Ltd. All rights reserved.

### 1. Introduction

Cenozoic paleoclimatic records within the Himalaya and Tibetan Plateau are sparse, but are needed to compare with the marine record of global climate changes for elucidating the role of Tibetan uplift in controlling regional and global climate (e.g., Kutzbach et al., 1989, 1993; Quade et al., 1989; Manabe and Broccoli, 1990; Harrison et al., 1992; Molnar et al., 1993; An et al., 2001; Molnar, 2005; Wang and Deng, 2005; Dupont-Nivet et al., 2007; Wang et al., 2008a). Intermontane basins in the Himalayan–Tibetan orogen often contain thick sequences of lacustrine and fluvial deposits with diverse fossils (Ji et al., 1980; CAS, 1989; Wang et al., 1996, 2006, 2008a; Yue et al., 2004; Horton et al., 2004). These sediments and fossils preserve a record of environmental changes in the region.

In this study, we determined the  $\delta^{13}\text{C}$  and  $\delta^{18}\text{O}$  values of lacustrine marls, carbonate cement and mammalian fossil material from late Miocene–Pliocene lacustrine and fluvial sediments in the Gyirong Basin on the north slope of the central Himalaya in southern Tibet (Fig. 1). We also performed X-ray diffraction analysis on selected sediment samples to determine their mineralogical components. The  $\delta^{18}\text{O}$  values of lacustrine carbonates record past changes in the  $\delta^{18}\text{O}$  of lake water and water temperature (e.g., Talbot, 1990; Dettman et al., 2003), which are controlled by regional climate and hydrology. Fluvial carbonates are generally believed to have formed by cementation of sediments due to percolation of shallow groundwater, and their oxygen isotopic compositions reflect the oxygen isotopic composition of shallow groundwater derived from local meteoric water (e.g., Dettman et al., 2003). Sediment clay mineralogy, on the other hand, helps to understand weathering conditions in the paleo-lake catchment that contributed sediment and water to the lake. Wang et al. (1996) reported limited carbonate  $\delta^{18}\text{O}$  data from about 40 lacustrine sediment samples from the

\* Corresponding author. Tel.: +1 850 644 1121; fax: +1 850 644 0827.

E-mail address: [ywang@magnet.fsu.edu](mailto:ywang@magnet.fsu.edu) (Y. Wang).

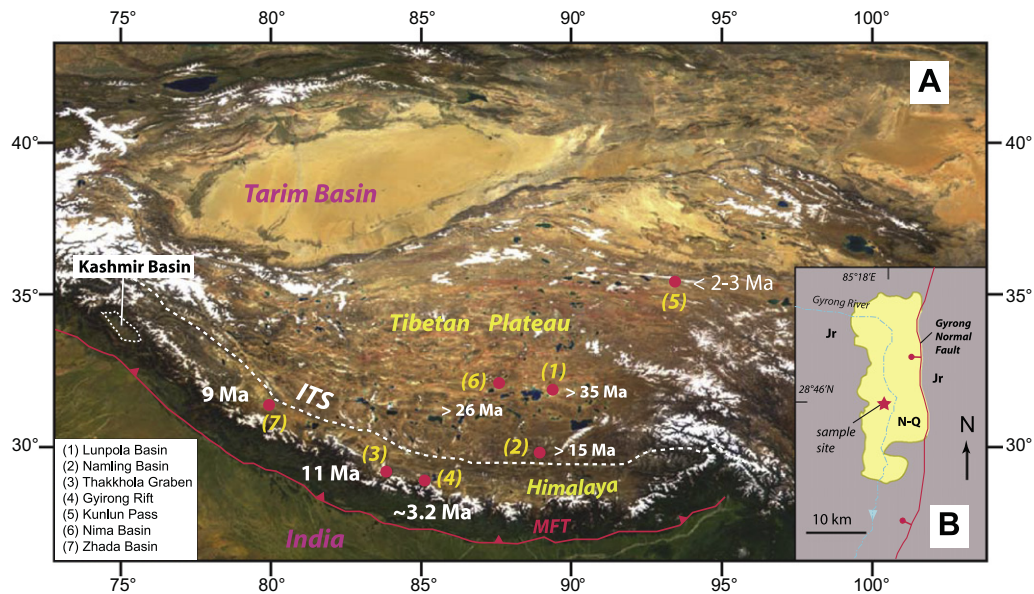


**Fig. 1.** LANDSAT image of the Tibetan Plateau and the Himalayan Range. (1)–(3), and (5)–(7) in (A) are sites with published paleo-elevation data (Garzione et al., 2000; Rowley and Currie, 2006; DeCelles et al., 2007; Spicer et al., 2003; Wang et al., 2008a; Saylor et al., 2009; Murphy et al., 2009). (4) is the site of this study – the Gyirong Basin which is shown in (B). ITS, Indus-Tsangpo suture zone; MFT, Main Frontal Thrust; N–Q, Neogene–Quaternary strata, and Jr, Jurassic strata. Ages in (A) indicate the times at which the region was thought to have reached its current elevation. It is important to note that the age of the Thakkhola graben was constrained using the *Hipparion* fauna found in the Gyirong Basin by assuming that the Thakkhola and Gyirong grabens were formed at about the same time and that the maximum age of the *Hipparion* fauna in the Gyirong Basin was  $\sim 10.7$  Ma (Garzione et al., 2000).

late Cenozoic sedimentary sequence in the Gyirong Basin and interpreted the large variations in their carbonate  $\delta^{18}\text{O}$  data (from  $-21.5\text{‰}$  to  $-10.9\text{‰}$ ) as reflecting climatic fluctuations in temperature. However, their interpretation is not viable because temperatures would have to vary by  $46\text{ °C}$  in order to produce this degree of carbonate- $\delta^{18}\text{O}$  variability for a given water source. Here, we report the isotope data from over 360 samples collected at 0.4–0.5 m sampling interval from the same sedimentary sequence in the Gyirong Basin. The high temporal resolution of our record permits a temporally detailed comparison of environmental changes in the area and possible forcing factors, such as tectonic events or global climate change. In addition, we applied a novel approach (Zanazzi et al., 2007) that combines *in vivo* oxygen isotope signatures of fossil enamel with diagenetic oxygen isotope compositions of fossil bones to reconstruct the paleo-temperatures and paleo-elevation of the basin in the latest Miocene. Our data provide new insight into the growth history of the Himalayan Range and Tibetan plateau and the role of global climate change in controlling local environmental conditions.

## 2. Geologic setting and modern climate of study site

The Gyirong Basin ( $28^{\circ}46.13'\text{N}$ ,  $85^{\circ}17.84'\text{E}$ ) is a late Cenozoic intermontane basin in the central Himalayas with an area of about  $200\text{ km}^2$  (Fig. 1). The basin is bounded by an active fault on the east and lies at elevations of 4100–4500 m above sea level (a.s.l.). It was suggested that the Gyirong Basin was originally an east–west trending grabben formed by the north–south extension related to the south Tibetan detachment system and was later deformed by the north–south trending normal fault to form the present north-trending valley (Yang et al., 2009). Sediment began to accumulate in the basin at  $\sim 7.2$ – $10.2$  Ma, as evidenced by the initial deposition of conglomeratic sediment on top of the Jurassic marine strata and beneath the Woma Formation – a thick sequence of lacustrine and fluvial sediments (Yue et al., 2004; Xu et al., this issue). Although there is no clear displacement between the sediments and the basement, the beddings were tilted to the north along the southern

boundary and to the east along the eastern boundary of the basin (Yang et al., 2009).

The present-day mean annual temperature in the Gyirong Basin is  $0$ – $3\text{ °C}$  and annual rainfall is about 230–370 mm (Sun et al., 2007). The climate in the area is influenced by the Indian monsoon, with the rainy season extending from June to September and the dry season from October to May (Tibet Bureau of Surveying and Mapping, 2000). The area is essentially a desert and has little vegetation except along the south-flowing Gyirong River (Fig. 1B).

The late Miocene–Pliocene Woma Formation is well exposed in the badlands in the modern Gyirong Basin (Figs. 2 and 3). A *Hipparion* fauna – a mammalian fossil assemblage containing the three-toed late Miocene–Pliocene horse *Hipparion* was found in the lower Woma Formation (Ji et al., 1980). The fauna is preserved in a red sandstone bed at an elevation of 4384 m a.s.l.,  $\sim 300$  m above the current valley floor, and includes the horse *Hipparion forstenae*, rhino *Chilotherium xizangensis*, artiodactyls *Metacervulus capreolinus*, *Palaeotragus microdon*, *Gazella gaudryi*, lagomorph *Ochotona guizhongensis*, rodent *Heterosminthus* sp., and carnivore *Hyaena* sp. (Ji et al., 1980; CAS, 1989). We interpret the fossil-bearing sandstone bed as overbank deposits by floodwaters in a fluvial setting of the paleo-lake basin. Diverse shell and plant fossils in the Woma Formation were reported by Ji et al. (1980), CAS (1989), and Sun et al. (2007). Although the Woma Formation is currently preserved in the Gyirong Basin, it is not clear if the sediments were deposited during the early developmental stage of the currently active Gyirong rift, or if the sediments have been preserved in the younger rift basin because the topographic depression has protected them from erosion. Because of this uncertainty in tectonic setting for the Woma Formation, we distinguish the paleo-Woma lake basin from the Gyirong Basin, with the former representing the latest Miocene to Pliocene lake basin of an unknown size, while the latter represents a Quaternary basin occupying the Gyirong valley (Fig. 1).

The Woma Formation is  $\sim 160$ -m thick (Fig. 3). It is composed of finely laminated lacustrine siltstone, sandstone, mudstone and marls, with a few interbedded sandstone layers of fluvial origin (Fig. 3; Yue et al., 2004). The sequence is capped by a conglomerate

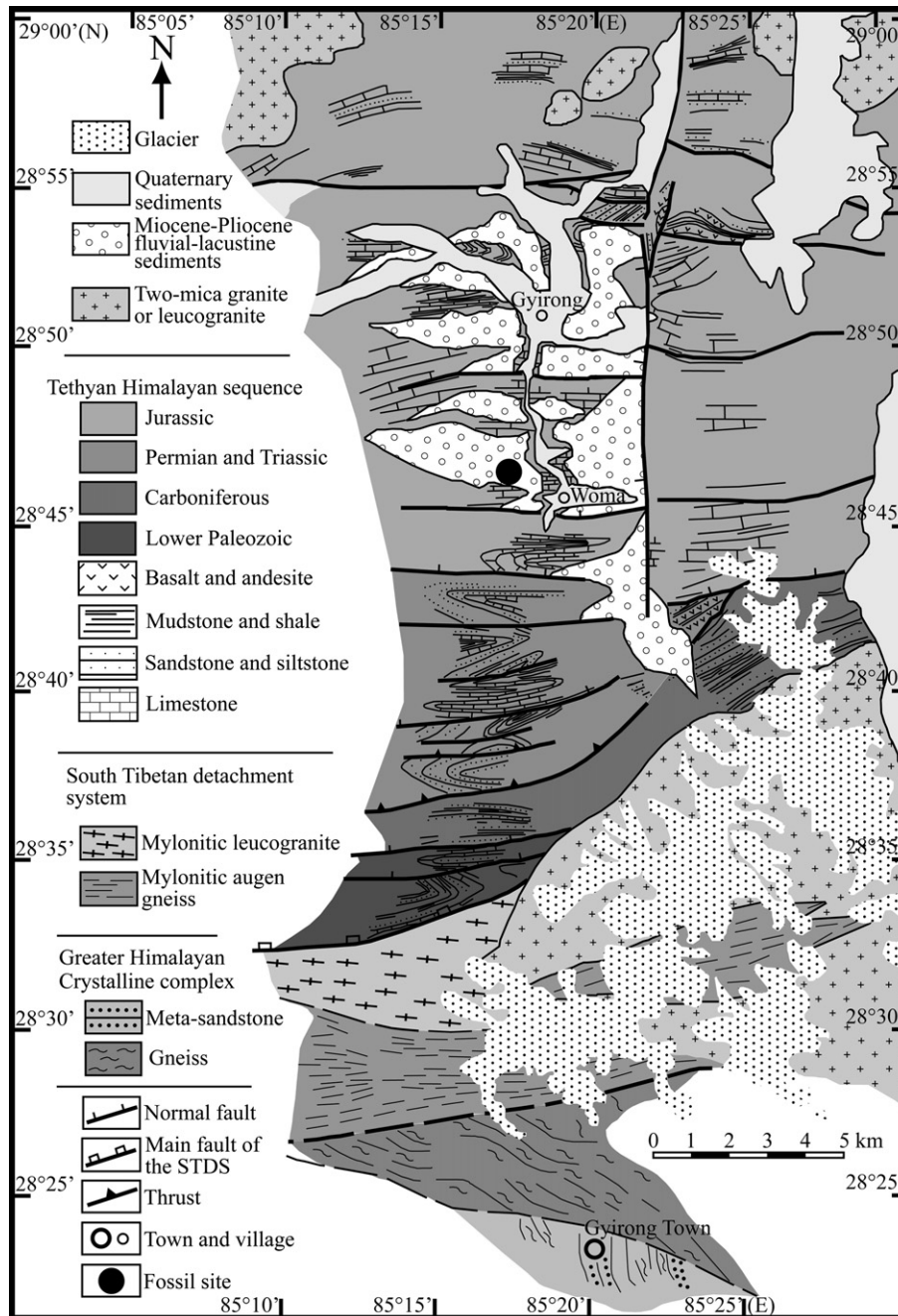


Fig. 2. Sketch geologic map the Gyirong Basin and surrounding area (adapted from Yang et al., 2009).

layer of ~2 m thick that signals the demise of the lake environment. Yue et al. (2004) collected two sets of parallel samples at ~0.45 m intervals throughout the 160 m section for paleomagnetic study. The paleomagnetic samples were subjected to natural remanent magnetization determinations and then thermally demagnetized at 50 °C, 100 °C, 150 °C, 200 °C, 250 °C, 300 °C, 350 °C, 400 °C, 450 °C, 500 °C, 550 °C, 600 °C, and 650 °C. Eighteen magnetic polarity zones were recognized in the Woma section, and the correlation with the standard geomagnetic polarity time scale was constrained by the *Hipparion* fauna (Yue et al., 2004). The resulting magnetostratigraphy (Fig. 3) suggests that the Woma Formation was deposited continuously from 7.2 Ma to 3.2 Ma, and the age of the *Hipparion* fauna is ~7 Ma (Yue et al., 2004).

In this study, we obtained a sub-sample of each of the original 368 paleomagnetic samples collected by Yue et al. (2004) as well

as fossil mammalian teeth from the Gyirong Basin for stable isotopic analyses. Our sediment samples were not subjected to thermal demagnetization treatment. Using the paleomagnetic data of Yue et al. (2004), the ages of our samples were linearly interpolated within this magnetostratigraphic framework (Fig. 3), yielding a record with a time resolution of ~11 thousand years (kyr).

### 3. Methods

Mineralogical components of selected sediments were determined by X-ray diffraction (XRD) analysis (Supplementary Table 1). Samples were suspended in high purity water and dried on zero-background holders for measurements on a Siemens D500 theta-2theta powder diffractometer. The mineral ratio is defined as the

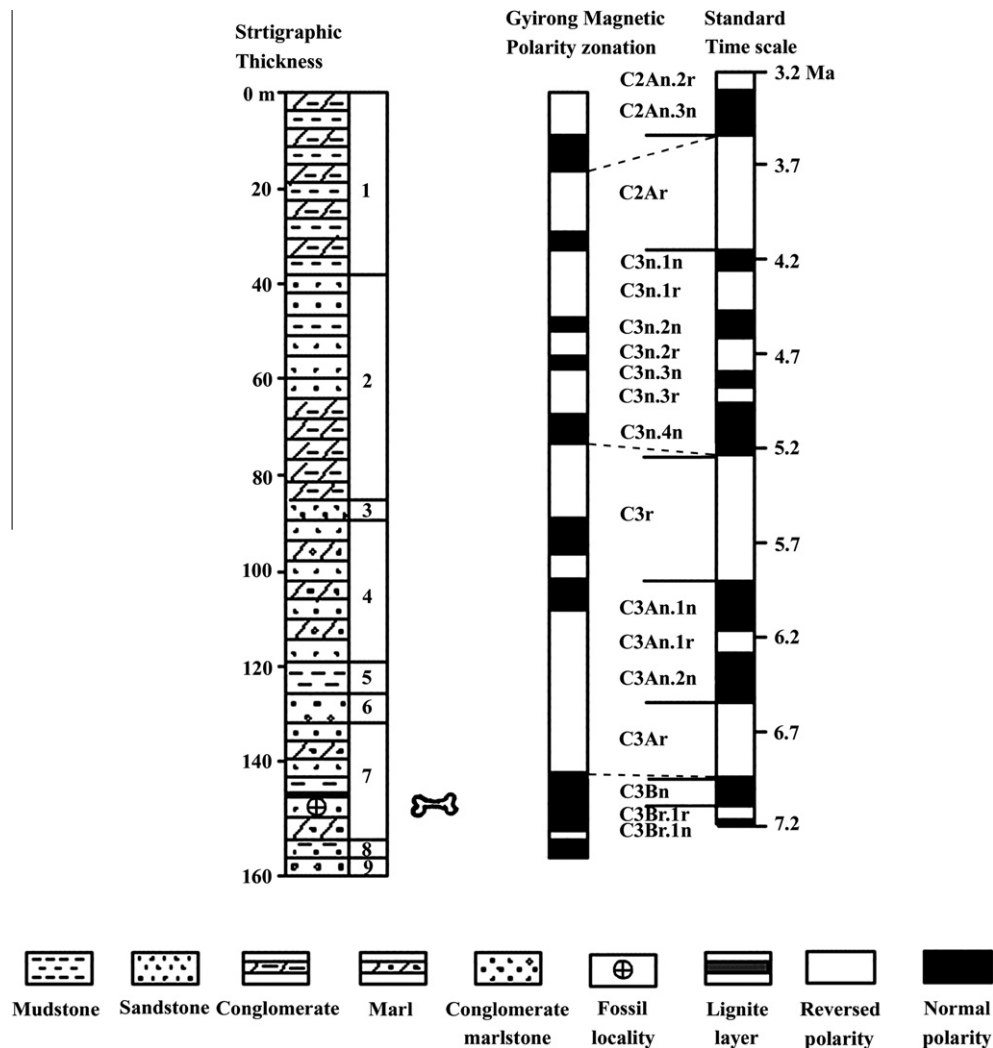


**Fig. 3.** The lithostratigraphy and magnetic stratigraphy of the Woma Formation in the basin (adapted from Yue et al., 2004). The Woma Formation is capped by a conglomerate layer of ~2 m thick (not shown). The age of the fossil mammalian fauna is determined on the basis of magnetostratigraphy and stratigraphic position.

ratio of intensities of XRD peaks characteristic of the minerals, which reflects the relative amounts of the two minerals in a sample. The data span 5–35° at 0.01° steps and a 1°/min scan rate. All 368 sediment samples were ground into fine powder for stable carbon and oxygen isotope analyses of carbonates (if present). The  $\delta^{18}\text{O}$  and  $\delta^{13}\text{C}$  values of carbonates were measured using a Gas Bench II Auto-carbonate device connected to a Finnigan MAT Delta Plus XP stable isotope ratio mass spectrometer (IRMS) at Florida State University. Powdered samples were reacted with 100% phosphoric acid at 25 °C overnight and the resulting  $\text{CO}_2$  was then introduced into the IRMS for carbon and oxygen isotopic measurements.

Teeth were sampled by drilling along the entire length of a tooth using a rotary drill to ensure that the sample would yield an integrated isotopic signal for the growth period of the tooth. For tooth fragments, the enamel was manually separated from the dentine and other matrix using a rotary tool and ground into a fine powder using a mortar and pestle. Fossil bones were ground to fine powder using a mortar and pestle. Any matrix that was initially present was manually removed from each sample prior to grinding. Fossil enamel and bone powders were soaked in 5% sodium hypochlorite (NaOCl) overnight to remove any possible organic contaminants, cleaned with distilled water and freeze-dried. The powder was then treated with 1 M acetic acid under weak vacuum overnight to remove carbonate, cleaned with dis-

tilled water and freeze-dried (Wang and Deng, 2005). With the exception of samples TB-4 to TB-12 (Supplementary Table 2) which were acidified at 25 °C over three nights and analyzed on a dual-inlet IRMS previously, the treated enamel samples were reacted with 100% phosphoric acid at 72 °C overnight and the carbon and oxygen isotopic ratios of the  $\text{CO}_2$  produced were analyzed using a Gas Bench II Auto-carbonate device connected to the IRMS. The isotopic data were calibrated based on measurements of at least two sets of three different carbonate (calcite) standards (including NBS-19 and two other lab standards) processed with each batch of sediment carbonates or enamel carbonate samples. Isotope data are reported in the standard notation as  $\delta^{13}\text{C}$  and  $\delta^{18}\text{O}$  in reference to the international carbonate standard VPDB (Pee Dee Belemnite) except water whose  $\delta^{18}\text{O}$  is in reference to the international standard VSMOW (standard mean ocean water). The analytical precision (based on replicate analyses of lab standards processed with each batch of samples) is  $\pm 0.1\text{‰}$  ( $1\sigma$ ) or better for both  $\delta^{13}\text{C}$  and  $\delta^{18}\text{O}$ .

As mentioned above, most of our fossil enamel samples in this study were acidified at 72 °C. In acid decomposition of carbonate, the liberated  $\text{CO}_2$  only contains two-thirds of the oxygen in the carbonate. As a consequence, the  $\delta^{18}\text{O}$  value of the evolved  $\text{CO}_2$  is always higher than in the original carbonate. A so-called “acid fractionation factor” must be applied to the measured  $\delta^{18}\text{O}$  value of the  $\text{CO}_2$  to obtain the  $\delta^{18}\text{O}$  value of the carbonate (Swart et al.,

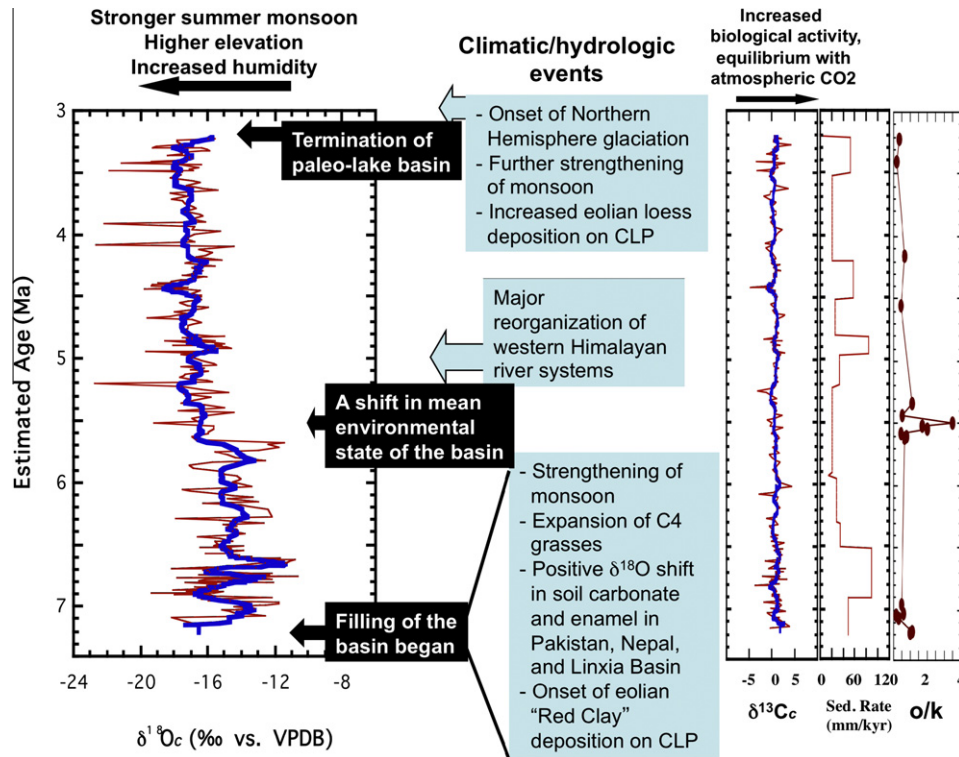


**Fig. 4.** The evolving oxygen and carbon isotopic compositions of lacustrine/fluvial carbonates, sedimentation rate, orthoclase/kaolinite (o/k) ratio, and paleo-lake basin environment in the Gyirong Basin in relation to known climatic/hydrologic events in Tibet and surrounding regions. The blue lines represent the 8-point-running average of the data. CLP = Chinese Loess Plateau.

1991). It is generally assumed that acid fractionation factor for calcite can be applied to structural carbonate in enamel bioapatite. However, Passey et al. (2007) recently showed that different acid reaction temperatures may result in isotopic discrepancies of up to 1.5‰ in reported enamel- $\delta^{18}\text{O}$  values because the carbonate component of enamel bioapatite is not the same as that of calcite as generally assumed. Because all our enamel- $\delta^{18}\text{O}$  data were calibrated using calcite standards, we have added 0.7‰ (i.e., the average per mil difference in  $\delta^{18}\text{O}$  between enamel samples reacted at 25 °C and 72 °C, see Fig. 4 in Passey et al., 2007) to normalize the data to acid reaction temperature of 25 °C to account for the difference in acid fractionation factor between calcite and structural carbonate in enamel bioapatite. Although this is a minor factor in the following interpretation, the normalization allows comparison of these data with other enamel data produced in our lab (as we now uniformly acidify samples at 25 °C) and with data from many other labs.

## 4. Results and Interpretation

### 4.1. Sediment mineralogy and stable isotope data

XRD analysis results show that the common minerals in the collected samples are quartz, calcite, illite, kaolinite, and orthoclase (or feldspar) (Supplementary Table 1 and Fig. 4). Some of the samples also contain vermiculite or chlorite as indicated by one low angle peak that is consistent with either phase.

The  $\delta^{13}\text{C}_c$  values of carbonates ( $\delta^{13}\text{C}_c$ ) are between  $-5\text{‰}$  and  $5\text{‰}$  throughout the sequence without any significant long-term trend (Fig. 4, Supplementary Table 2), possibly reflecting variations in biological productivity in the lake or equilibrium with atmospheric  $\text{CO}_2$  (e.g., Talbot, 1990). In contrast, the  $\delta^{18}\text{O}_c$  values of carbonates ( $\delta^{18}\text{O}_c$ ) range from  $-10.7\text{‰}$  to  $-22.8\text{‰}$ , with an abrupt change in the long-term trend at  $\sim 5.64\text{--}5.50\text{ Ma}$  (Fig. 4). Although the lim-

ited data reported by Wang et al. (1996) fall within the  $\delta^{18}\text{O}_c$  range of our data, it is impossible to directly compare their record with ours due to inconsistency in the perceived magnetozones. Late diagenesis did not modify the isotopic composition of the carbonates, because this would have shifted the  $\delta^{18}\text{O}_c$  to more negative values with increasing burial depth (due to elevated temperature), which is not seen in our data (Fig. 4). The high amplitude variations preserved in the  $\delta^{18}\text{O}_c$  record (Fig. 4) also argue against significant diagenetic alteration of the isotopic compositions of the carbonates, as alteration would have greatly reduced the amplitude of  $\delta^{18}\text{O}_c$  variability. The preservation of  $\delta^{18}\text{O}$  variance at Milankovitch frequencies as discussed below provides additional evidence for limited (if any) diagenetic alteration of the isotopic compositions of the carbonates.

The  $\delta^{18}\text{O}_c$  of authigenic carbonate in lacustrine or fluvial sediments is determined by two variables: (1) the  $\delta^{18}\text{O}$  of water ( $\delta^{18}\text{O}_w$ ) (i.e., lake water or shallow groundwater) from which the carbonate is formed and (2) the temperature of carbonate formation (e.g., Talbot, 1990; Dettman et al., 2003). The  $\delta^{18}\text{O}_w$  value of lake water often deviates significantly from that of precipitation feeding the lake system due to evaporative enrichment in the heavy oxygen isotope  $^{18}\text{O}$  (Talbot, 1990; Fontes et al., 1996). Thus, the interpretation of terrestrial carbonate  $\delta^{18}\text{O}_c$  data is not straightforward as it is difficult to tease apart how much of the  $\delta^{18}\text{O}_c$  variation is due to changes in temperature, source (meteoric) water  $\delta^{18}\text{O}_w$ , and degree of evaporative  $^{18}\text{O}$  enrichment. Lack of strong covariance between  $\delta^{13}\text{C}_c$  and  $\delta^{18}\text{O}_c$  ( $r = 0.1907$  for 7.2–5.5 Ma;  $r = 0.3751$  for 5.5–3.2 Ma) suggests that the paleo-lake was not a closed system (i.e., internally drained lake) (Talbot, 1990).

### 4.2. Spectral analysis and interpretation of the $\delta^{18}\text{O}_c$ record

The most prominent feature of the  $\delta^{18}\text{O}_c$  record from the Woma Formation in the Gyirong Basin is an abrupt and statistically signif-

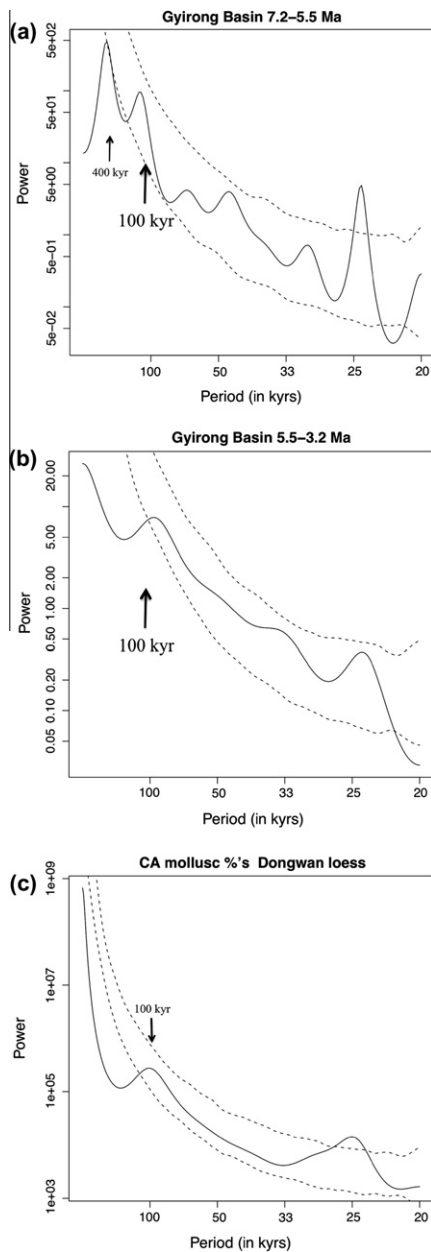


**Fig. 5.** Spectral analyses of  $\delta^{18}\text{O}$  values from older (a) and younger (b) portions of Gyirong sedimentary sequence and of cold-aridiphilous (CA) mollusk percentages (c) from the Dongwan loess sequence (from Li et al., 2008). Maximum entropy spectral analyses were performed using routine “spec.ar” in R version 2.10.1 (R-project, R Development Core Team, 2009). Lower dashed line in each figure represents the 95% confidence interval calculated using method of PPPHALOS software (Guiot and Goeury, 1996, as used in Li et al., 2008); and the upper dashed line is the 95% confidence interval calculated using analysis of 1000 random permutations of the original data.

icant shift to more negative values at  $\sim 5.64$ – $5.50$  Ma ( $t$ -test,  $t = 13.675$ , d.f. = 267, M.D. = 2.4,  $P < 0.0001$ ; Wilcoxon rank sum test,  $w = 24,842$ ,  $P < 0.0001$ ) (Fig. 4). This  $\delta^{18}\text{O}_c$  shift seems to reflect a major change in the mean environmental conditions of the basin and divides the  $\delta^{18}\text{O}_c$  record into two distinct periods (Fig. 4):

#### 4.2.1. $\sim 7.2$ . to $\sim 5.5$ Ma

During this first stage of basin development, the environment of the paleo-Woma lake was relatively stable with no significant change in the long-term  $\delta^{18}\text{O}_c$  trend (regression slope insignifi-

cantly different from zero), despite large fluctuations in the  $\delta^{18}\text{O}_c$  values (Fig. 4). The  $\delta^{18}\text{O}_c$  fluctuated around a mean value of  $-14.7 \pm 1.8\text{‰}$  ( $n = 153$ , all means reported  $\pm 1\sigma$ ), ranging from  $-10.7\text{‰}$  to  $-19.4\text{‰}$ . The average sedimentation rate for this time interval is about  $60 \pm 28$  mm/kyr. The fluctuations in the  $\delta^{18}\text{O}_c$  values likely reflect variations in regional water balance (i.e., evaporation vs. precipitation) or alternation between wetter and drier climate induced by orbital forcing, with relatively enriched  $\delta^{18}\text{O}_c$  values indicating drier periods or increased evaporation/precipitation (E/P) ratio (e.g., Hodell et al., 1991; Yu and Eicher, 1998; Wei and Gasse, 1999). Orbital forcing may be related to eccentricity and precession cycles based on a time series analysis (maximum entropy and lomb spectral analysis routines in R-project, R Development Core Team, 2009; and wavelet analysis, Torrence and Compo, 1998) of the  $\delta^{18}\text{O}_c$  values of our analyzed samples using sample ages linearly interpolated from paleo-magnetic dates of Yue et al. (2004). These analyses reveal strong 24 and 100 kyr cycles (with 95% confidence level) (Fig. 5a) which are consistent with the Milankovitch frequency bands of precession (23 ky) and eccentricity (100 ky) and also compare well with the 25 kyr and the 100 kyr cycles reported by Li et al. (2008) from the western Chinese Loess Plateau (Fig. 5a and c), implying that the large  $\delta^{18}\text{O}$  fluctuations during this time period are likely controlled by orbitally induced variations in climate.

#### 4.2.2. $\sim 5.5$ . to $\sim 3.2$ Ma

After an abrupt shift at  $\sim 5.64$ – $5.50$  Ma, the paleo-lake basin attained another relatively stable state (with no substantial change in the long-term  $\delta^{18}\text{O}_c$  average; regression slope  $0.000037 \delta^{18}\text{O}_c/\text{kyr}$ ,  $p = 0.008$ ) until  $\sim 3.2$  Ma, despite alternation between wetter and drier periods as indicated by large fluctuations in  $\delta^{18}\text{O}_c$  values (Fig. 4). During this second stage of basin development from  $\sim 5.5$  to  $3.2$  Ma, the  $\delta^{18}\text{O}_c$  values varied between  $-14.4\text{‰}$  and  $-22.8\text{‰}$ , with a mean of  $-17.1 \pm 1.3\text{‰}$  ( $n = 188$ ) that is  $2.4\text{‰}$  lower than the mean  $\delta^{18}\text{O}_c$  for the previous period. The average sedimentation rate is  $45 \pm 22$  mm/kyr, lower than the preceding time interval. Time series analysis, applied in a fashion similar to that discussed for the 7.2–5.5 Ma samples, revealed much less pronounced 24 and 100 kyr cycles (Fig. 5b), possibly due to reduced cycle amplitude or insufficient length of record.

The abrupt shift to more negative  $\delta^{18}\text{O}_c$  at  $\sim 5.64$ – $5.50$  Ma could imply a significant change in temperature. Temperature change affects the  $\delta^{18}\text{O}_c$  of freshwater carbonate in two ways: (1) by affecting the oxygen isotope fractionation between carbonate and water and (2) by affecting the  $\delta^{18}\text{O}_w$  of source water (i.e., meteoric water). The oxygen isotope fractionation between calcite and water varies by about  $-0.23\text{‰}$  per  $1^\circ\text{C}$  increase in temperature (Kim and O’Neil, 1997). At mid to high latitudes, there is a strong positive correlation ( $0.58\text{‰}/^\circ\text{C}$ ) between precipitation  $\delta^{18}\text{O}_w$  and surface air temperature (Dansgaard, 1964; Rozanski et al., 1993), but this correlation is much weaker or non-existent in low latitudes and in the Asian monsoon region where our study site is located (Dansgaard, 1964; Rozanski et al., 1993; Johnson and Ingram, 2004; Vuille et al., 2005). If the temperature effect on precipitation- $\delta^{18}\text{O}_w$  was also insignificant in the study area in the late Miocene, the negative shift of  $2.4\text{‰}$  in the mean  $\delta^{18}\text{O}_c$  values would require an overall  $11^\circ\text{C}$  warming (relative to the previous period) that persisted for over 2 million years following the 5.5-Ma event, inconsistent with the global climate trend that shows only a subtle warming during the early Pliocene relative to the latest Miocene (e.g., Lear et al., 2000; Zachos et al., 2001). If we assume that the precipitation-temperature relationship ( $0.58\text{‰}/^\circ\text{C}$ ) observed in mid to high latitudes today existed in the late Miocene in the Tibetan region, which would imply a net temperature effect of  $0.35\text{‰}/^\circ\text{C}$  on  $\delta^{18}\text{O}_c$ , the negative shift of  $2.4\text{‰}$  in the mean  $\delta^{18}\text{O}_c$  values in the Woma Formation would require an overall  $7^\circ\text{C}$  cooling that

persisted for over 2 million years following the 5.5-Ma event, which is also inconsistent with the global and regional climate trend (e.g., Lear et al., 2000; Zachos et al., 2001 and discussion below). Thus, a change in temperature cannot explain this negative  $\delta^{18}\text{O}_c$  shift. Alternatively, if meteoric water  $\delta^{18}\text{O}_w$  remained the same, the more negative  $\delta^{18}\text{O}_c$  values for the period of  $\sim 5.5$ – $3.2$  Ma could reflect a reduced E/P ratio, implying either (1) a wetter climate or a stronger summer monsoon in the region during this time period compared to the previous interval of  $7.2$ – $5.5$  Ma or (2) a decrease in water residence time in the lake due to faster passage of stream water through the lake. However, the inference of a wetter climate is inconsistent with other evidence for a drying climate in Asia since  $\sim 8$ – $9$  Ma (e.g., Barry and Flynn, 1990; Barry et al., 2002; Quade et al., 1989, 1995; An et al., 2001; Saylor et al., 2010). A change in residence time is also unlikely cause because this  $\delta^{18}\text{O}_c$  shift occurred over a much longer time scale (Fig. 4) than the isotopic response time of a lake (i.e., a few years to a few decades) to a change in residence time (Wei and Gasse, 1999). Furthermore, if the lake had become more open and yet the paleo-meteoric water had maintained the same  $\delta^{18}\text{O}_w$  value as that of today, the most negative  $\delta^{18}\text{O}_c$  value of  $-22.8\text{‰}$  after 5.5 Ma (Fig. 4) would require that the carbonate was formed at an unreasonably high temperature of about  $40^\circ\text{C}$ . Thus, a reduced E/P value without any significant change in the  $\delta^{18}\text{O}_w$  of meteoric water throughout the past 7 million years also cannot explain the 5.5-Ma  $\delta^{18}\text{O}_c$  shift.

It appears that the only plausible explanation for this 5.5-Ma  $\delta^{18}\text{O}_c$  shift is a change in the  $\delta^{18}\text{O}_w$  of meteoric water in the catchment feeding the paleo-lake basin. The  $\delta^{18}\text{O}_c$  data from the Gyirong Basin, just like the  $\delta^{18}\text{O}_c$  data from other basins in the Himalayan–Tibetan region (e.g., Garzzone et al., 2000; Rowley and Currie, 2006; Saylor et al., 2009), show a large range ( $>10\text{‰}$ ) of variation. The most negative  $\delta^{18}\text{O}_c$  values of lacustrine and other terrestrial carbonates have been widely used to infer the  $\delta^{18}\text{O}_w$  of paleo-meteoric water and paleo-elevation (e.g., Garzzone et al., 2000; Dettman et al., 2003; Rowley and Currie, 2006; Rowley and Garzzone, 2007; DeCelles et al., 2007; Murphy et al., 2009; Saylor et al., 2009) as evaporation increases the  $\delta^{18}\text{O}$  of lake/soil water and likewise the carbonates. The most negative  $\delta^{18}\text{O}_c$  value after 5.5 Ma is  $-22.8\text{‰}$ , which is  $3.4\text{‰}$  more negative than the lowest value of  $-19.4\text{‰}$  for the previous period. That is, not only is the mean  $\delta^{18}\text{O}_c$  value significantly lower, but also the most negative  $\delta^{18}\text{O}_c$  value, after the 5.5-Ma event, is considerably lower. Therefore, we interpret this 5.5-Ma  $\delta^{18}\text{O}_c$  shift as indicating a decrease in the  $\delta^{18}\text{O}_w$  of meteoric water in the catchment area of the paleo-Woma lake due to a significant change in the mean environmental state of the paleo-lake basin.

#### 4.3. $\delta^{18}\text{O}$ of mammalian teeth and bones, and paleotemperature and paleoelevation interpretations

The  $\delta^{18}\text{O}$  values of fossil teeth and bones from the *Hipparion* fauna found in the lower Woma Formation are reported in Supplementary Table 3. The  $\delta^{18}\text{O}$  values of enamel samples from fossil horses and rhinos range from  $-11.1\text{‰}$  to  $-18.0\text{‰}$ , with a mean of  $-16.4 \pm 1.4\text{‰}$  ( $\pm 1\sigma$ ,  $n = 41$ ). The  $\delta^{18}\text{O}(\text{CO}_3^{2-})$  values of fossil mammalian bones collected from the same fossil locality ( $\sim 7$  Ma) are  $-17.8\text{‰}$  to  $-19.5\text{‰}$ , with a mean of  $-18.8 \pm 0.5\text{‰}$  ( $\pm 1\sigma$ ,  $n = 10$ ). Modern enamel samples from horses and yaks from the Gyirong Basin yielded  $\delta^{18}\text{O}$  values of  $-12.4\text{‰}$  to  $-20.0\text{‰}$  (Wang et al., 2008b), averaging  $-15.3 \pm 2.1\text{‰}$  ( $n = 76$  enamel samples from 31 teeth).

Early studies suggested that the *Hipparion* fauna in the Gyirong Basin, which was dated magnetostratigraphically at  $\sim 7$  Ma (Fig. 3), resembled assemblages in northern China, representing a mixed habitat of woodlands and grasslands, and that the local ele-

vation at that time would have been significantly less, at  $\sim 500$ – $1000$  m a. s. l. (e.g., Ji et al., 1980; CAS, 1989). A recent stable carbon isotopic study of this fauna (Wang et al., 2006) reveals that these ancient mammals, unlike modern herbivores in the area, ate significant amounts of  $\text{C}_4$  grasses (i.e., warm climate grasses). In the modern world,  $\text{C}_4$  grasses are mostly confined to low altitudes and latitudes (Hofstra et al., 1972; Tieszen et al., 1979; Boutton et al., 1980; Li et al., 2009; Edwards et al., 2010). Although  $\text{C}_4$  grasses have been found in the warmest months in southern Tibet, they account for negligible amounts of the biomass (e.g., Lu et al., 2004; Wang et al., 2008b; Li et al., 2009). The presence of significant  $\text{C}_4$  grasses in the diets of these ancient herbivores ( $\sim 30$ – $70\%$   $\text{C}_4$ ) was interpreted by Wang et al. (2006) as indicating significant  $\text{C}_4$  biomass in the paleo-Woma lake basin in the latest Miocene. This is consistent with paleosol carbonate  $\delta^{13}\text{C}$  data from the nearby Thakkhola graben (Garzzone et al., 2000) that indicate the existence of  $\text{C}_4$ -dominated grasslands with  $\text{C}_4$  grasses accounting for as high as 100% of the biomass in the area in the latest Miocene. Thus, the carbon isotope data suggest a much warmer and wetter climate in the Gyirong-Thakkhola area at about 7 Ma than today (Wang et al., 2006), in agreement with the habitat inferred from the fossil assemblage contained in the same layer (Ji et al., 1980; CSA, 1989). Furthermore, the carbon isotope data provide a constraint on the paleo-elevation of the area in the latest Miocene, suggesting that the basin was no more than 2900–3400 m a.s.l. at  $\sim 7$  Ma (Wang et al., 2006). Analyses of pollen assemblages in the Woma Formation revealed a rich and diverse flora (ranging from trees, grasses to furs) including tropical and subtropical plants such as *Osmunda*, *Pteris*, and *Polypodiaceae* in the paleo-Woma lake basin, which also indicates a much warmer and wetter climate, and thus lower elevation of the basin, in the late Miocene than today (Sun et al., 2007; Xu et al., this issue).

Recent studies suggest that the  $\delta^{18}\text{O}$  of fossil bone carbonate is reset completely during early diagenesis on time scales of 20–50 kyr (Kohn and Law, 2006). Thus, the  $\delta^{18}\text{O}$  of the fossil bone carbonate reflects the  $\delta^{18}\text{O}_w$  of local meteoric water and local mean annual air temperature, and could serve as a paleo-thermometer if the  $\delta^{18}\text{O}_w$  could be estimated from the  $\delta^{18}\text{O}$  of fossil mammalian tooth enamel (Kohn and Law, 2006; Zanazzi et al., 2007). The underlying assumptions associated with this paleo-thermometry approach (Zanazzi et al., 2007) are: (1) bone carbonate records early diagenetic (i.e., pedogenic) conditions and its  $\delta^{18}\text{O}$  composition reflects local mean annual temperature and the  $\delta^{18}\text{O}_w$  of local meteoric water, and (2) the  $\delta^{18}\text{O}_w$  of local meteoric water can be determined from the  $\delta^{18}\text{O}$  of fossil enamel (i.e., the water ingested by the animals is isotopically the same as the water in which the bones fossilized). Here, we apply this fossil-based paleo-thermometer to the  $\delta^{18}\text{O}$  of fossil teeth and bones from the *Hipparion* fauna found in the Woma Formation (Fig. 3) in an attempt to reconstruct the paleo-temperatures and paleo-elevation of the paleo-Woma lake basin.

Studies have shown that the enamel- $\delta^{18}\text{O}$  values of obligate drinkers are strongly correlated with the  $\delta^{18}\text{O}_w$  of meteoric water (e.g., Kohn and Cerling, 2002; Levi et al., 2006). Applying the enamel–water  $\delta^{18}\text{O}$  relationship for obligate drinkers given in Kohn and Cerling (2002) (i.e.,  $\delta^{18}\text{O}_{\text{enamel-PO4}} = 0.9 \delta^{18}\text{O}_{\text{water}} + 23$  or  $\delta^{18}\text{O}_{\text{enamel-CO3}} = 0.9 \delta^{18}\text{O}_{\text{water}} + 1.245$ ) to modern enamel samples from horses and yaks yielded an average meteoric water  $\delta^{18}\text{O}_w$  value of  $-18.6 \pm 2.1\text{‰}$  (vs. VSMOW), which is almost the same as the  $\delta^{18}\text{O}_w$  value of the present-day local tap water ( $-18.4\text{‰}$  vs. VSMOW) collected in 2004 (Supplementary Table 3). Similarly, we estimated the average  $\delta^{18}\text{O}_w$  of paleo-meteoric water from the  $\delta^{18}\text{O}$  values of enamel from fossil horses and rhinos found in the Gyirong Basin using the enamel–water  $\delta^{18}\text{O}$  relationship of Kohn and Cerling (2002). The estimated  $\delta^{18}\text{O}_w$  values of paleo-meteoric water in the late Miocene are  $-19.6 \pm 1.5\text{‰}$  ( $\pm 1\sigma$ ,

$n = 42$ ), slightly lower than that of the present-day local water. Using the approach of Zanazzi et al. (2007), we calculated the paleo-temperatures for the latest Miocene (Fig. 6; Supplementary Table 4) from the estimated local-water  $\delta^{18}\text{O}_w$  values, the apparent enrichment factor ( $\sim 2.2\text{‰}$ ) between bone carbonate (i.e., francolite) and soil carbonate (calcite) (Kohn and Law, 2006), and the  $\delta^{18}\text{O}$  values of fossil bone carbonates using the general oxygen isotope fractionation factor and temperature equation (Kim and O'Neil, 1997). The estimated mean annual temperature (MAT) at  $\sim 7$  Ma in the Gyirong Basin is  $21 \pm 6$  °C (Fig. 6a), which is about 19 °C higher than the present-day MAT of 2 °C in the basin (Fig. 6b).

The average  $\delta^{18}\text{O}_c$  value of lacustrine carbonates at 6.9–7.1 Ma is  $-15.2 \pm 2.0\text{‰}$ . Using the paleo-temperature estimated above from fossils, we calculated the average  $\delta^{18}\text{O}_w$  value of lake water in equilibrium with these lacustrine carbonates to be  $-14 \pm 2\text{‰}$ , which is higher than that of paleo-meteoric water estimated from fossil enamel. This isotopic difference is consistent with what is expected of evaporated lake water as evaporation preferentially removes isotopically lighter water molecules leaving remaining water enriched in the heavy oxygen isotope  $^{18}\text{O}$  relative to source (meteoric) water (e.g., Gonfiantini, 1986).

Marine Mg/Ca records suggest that the ocean temperatures  $\sim 7$  Ma were about 2–3 °C higher than today (Lear et al., 2000). However, temperature changes at high elevations are larger (maybe two times) than at sea level (Bradley et al., 2004, 2006). If we assume that late Cenozoic global cooling has resulted in a temperature drop of 5 °C (about twice that at sea level) in the Gyirong Basin since  $\sim 7$  Ma, the estimated temperature change in the basin would suggest an elevation change of  $2414 (\pm 1034)$  m since that time using the following equation and the present-day temperature gradient of  $-5.8$  °C/km in the region determined from the modern elevation/temperature data of Gyirong County ( $28.77^\circ\text{N}$ ,  $85.30^\circ\text{E}$ ,  $\sim 4200$  m a.s.l., MAT = 2 °C) and New Delhi (similar latitude,  $28.58^\circ\text{N}$ ,  $77.20^\circ\text{E}$ , 211 m a.s.l., MAT = 25.0 °C):

$$\text{Elevation change} = (T_{LM} - T_M - \Delta T) / 5.8 \text{ °C} / 1000 \text{ m} \quad (1)$$

where  $T_{LM}$  is the estimated temperature at  $\sim 7$  Ma,  $T_M$  is the modern temperature, and  $\Delta T$  the local temperature change due to global cooling since the late Miocene. The uncertainty in the paleo-elevation estimate corresponds to the uncertainty in paleo-temperature ( $\pm 6$  °C), which accounts for the uncertainty in paleo-water  $\delta^{18}\text{O}$  and the  $\delta^{18}\text{O}$  variability of fossil bone carbonates. If the paleo-temperature derived from the fossil-based  $\delta^{18}\text{O}$  “paleo-thermometer” (Zanazzi et al., 2007) did not approximate the MAT but were biased to the growing season temperature that could be 5–6 °C higher than the MAT, the above calculation would lead to an overestimation of the elevation change by up to 1 km.

Subtracting the estimated elevation change from the current elevation of the fossil locality (4384 m a.s.l.) yielded a paleo-elevation of  $\sim 1970 \pm 1034$  m a.s.l. This implies that the elevation of the paleo-Woma lake basin in the latest Miocene was significantly lower than its present-day elevation (Fig. 6b). If we use the present-day atmospheric lapse rate of  $-6.5$  °C/km, the estimated temperature change since the latest Miocene would correspond to an elevation change of  $2154 \pm 923$  m, implying that the paleo-lake basin was about  $2230 \pm 923$  m a.s.l. at  $\sim 7$  Ma. Whatever lapse rates used, these temperature-based paleo-elevation estimates (despite large uncertainties) are consistent with fossil evidence (Hsu, 1976; Ji et al., 1980; CAS, 1989; Sun et al., 2007; Xu et al., this issue) and the carbon isotope data (Wang et al., 2006), indicating that the paleo-Woma lake basin in the Gyirong area and possibly a significant portion of the central Himalaya were at a much lower elevation than today.

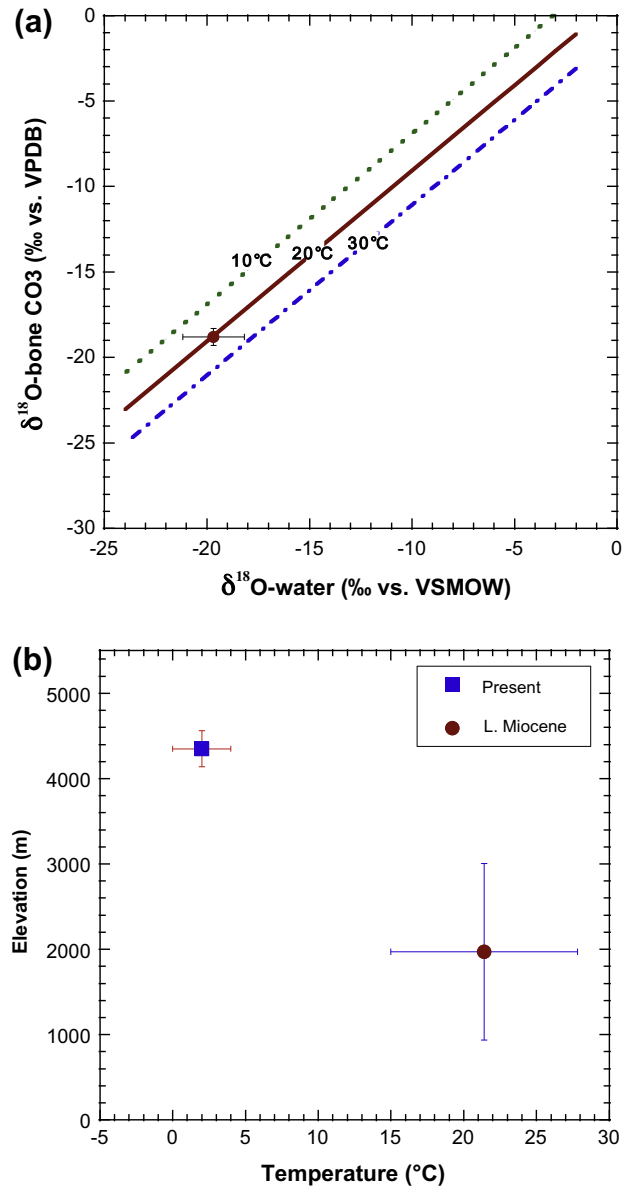


**Fig. 6.** Estimates of paleo-temperatures based on the  $\delta^{18}\text{O}$  values of diagenetic fossil bone carbonates and paleo-water in the latest Miocene (a), and paleo-elevation of the Gyirong Basin calculated from estimated temperature change in the basin since  $\sim 7$  Ma (b). The solid dot represents the mean paleo-temperature estimated for the latest Miocene. The lines in (a) represent expected equilibrium  $\delta^{18}\text{O}$  relationships between fossil bone carbonate and water, calculated using a new fossil-based oxygen isotope “paleo-thermometer” (Kohn and Law, 2006; Zanazzi et al., 2007; see text for explanation).

## 5. Discussion

### 5.1. Evolution of the paleo-lake system

The filling of the basin began at  $\sim 7$ –10 Ma (Yue et al., 2004; Xu et al., this issue), and likely marks the initiation of north-trending rifting in the area or formation of a major topographic barrier south of the Gyirong basin induced by Himalayan thrusting (i.e., a piggy-back basin in a thrust hanging wall). This local environmental event is broadly synchronous with the onset of nearby normal faulting in southern Tibet at about 5–9 Ma (Harrison et al., 1995; Murphy et al., 2002; Maheo et al., 2007). However, we do note that this event is younger than the 14–16 Ma onset ages of rifting recorded in northern and western Tibet (Jolivet et al., 2003; Blisniuk et al., 2001; Lacassin et al., 2004; Thiede et al., 2006). Other “coe-

val" ( $\sim 8 \pm 1$  Ma) environmental changes have also been documented in areas surrounding the plateau (Fig. 4), including the strengthening or onset of the Indian monsoon as inferred from changes in foraminiferal assemblages in the Arabian Sea (e.g., Kroon et al., 1991; Molnar et al., 1993), the expansion of  $C_4$  grasses in the Indian subcontinent (Quade et al., 1989, 1992, 1995), the onset of widespread "Red Clay" deposition on the Chinese Loess Plateau (An et al., 2001), and a shift to a drier climate as indicated by positive  $\delta^{18}O$  shifts in soil carbonates and tooth enamel in the Indian subcontinent and in the Linxia basin in northwest China (Quade et al., 1989, 1992, 1995; Wang and Deng, 2005). These various lines of evidence suggest a possible link between tectonic change and regional and global climate change (Quade et al., 1995; An et al., 2001).

The paleo-lake disappeared at  $\sim 3.2$  Ma as indicated by the deposition of fluvial-alluvial conglomerate on top of the Woma Formation (Fig. 3). This event is broadly coeval with a major reorganization of drainage network in eastern Himalayan river systems at  $\sim 3$ – $4$  Ma inferred from provenance analysis of detrital zircons in the eastern Himalayan rivers and foreland basin sediments (Cina et al., 2009), but slightly precedes a major change in the global climate system (Fig. 4) as marked by the onset of large Northern Hemisphere glacial/interglacial cycles (Shackleton et al., 1984; Maslin et al., 1998; Sossian and Rosenthal, 2009), strengthened monsoon circulation and increased loess deposition on the Chinese Loess Plateau (An et al., 2001). Although widespread Plio-Pleistocene deposition of conglomerate near the northern margin of the Tibetan Plateau has traditionally been interpreted as indicative of recent uplift of the plateau (e.g., Liu et al., 1996; Zheng et al., 2000), Zhang et al. (2001) argue that increases in sedimentation rate and grain size of sediments since 2–4 Ma (also observed in other mountainous regions) may be a global phenomenon related to a changed global climatic condition (from a stable climate to one with frequent, high-amplitude variations). In the paleo-Woma lake basin, the deposition of conglomerate (typical of alluvial fan debris deposits) at  $\sim 3.2$  Ma marks the end of the long depositional history of the paleo-lake basin (Figs. 3 and 4), more likely caused by tectonics that completely changed the depositional setting in the Gyirong area.

During the time period of the lake's existence, local climate fluctuated between wetter and drier conditions, possibly due to orbital forcing (Figs. 4 and 5). A major change in the mean environmental state of the paleo-Woma lake basin occurred at  $\sim 5.5$  Ma (Fig. 4) and was associated with an abrupt reduction in the  $\delta^{18}O_w$  of meteoric water in the catchment (see Section 4.2). Below we discuss possible causes for such an abrupt reduction in the  $\delta^{18}O_w$  of meteoric water in the catchment feeding the paleo-lake.

### 5.2. Cause of the $\delta^{18}O$ shift at $\sim 5.5$ Ma

A change in the  $\delta^{18}O$  of seawater (the ultimate source of meteoric water) does not appear to be sufficient to cause the significant reduction in the  $\delta^{18}O$  of meteoric water in the paleo-Woma lake basin at  $\sim 5.5$  Ma, as the  $\delta^{18}O$  record from marine benthic foraminifera shows little change during the latest Miocene-early Pliocene until  $\sim 3$  Ma when extensive Northern Hemisphere glaciation commenced and the  $\delta^{18}O$  of the ocean increased (Lear et al., 2000; Zachos et al., 2001). Other likely end-member explanations include: (1) intensified summer monsoon, (2) a significant reorganization of drainage systems in the central Himalaya that increased the mean elevation of the catchment or led to a catchment with a larger proportion of surface water sources at higher elevations than prior to  $\sim 5.5$  Ma.

The Himalayas are within the Indian monsoon regime. Modern precipitation in the Asian summer monsoon region displays a large range of  $\delta^{18}O$  variations strongly correlated with precipitation amount – the so-called "amount effect" (Dansgaard, 1964). The

precipitation amount in the region is primarily controlled by monsoon intensity (Johnson and Ingram, 2004; Vuille et al., 2005), with summer precipitation showing considerably lower  $\delta^{18}O$  values (due to greater amounts of precipitation) than winter precipitation. If similar effects controlled the  $\delta^{18}O$  of precipitation in the latest Miocene and Pliocene, an intensified summer monsoon that persisted for about 2 million years following the 5.5-Ma event would be required to allow for source (meteoric) water  $\delta^{18}O_w$  values to have decreased to the post-5.5 Ma values. This would also imply a wetter climate compared to the previous period. There is substantial evidence from both marine and terrestrial records for a strong monsoon circulation since  $\sim 7$ – $9$  Ma, but the existing data do not indicate further strengthening of the Indian monsoon at  $\sim 5.5$ – $3.2$  Ma (Burkle, 1989; Kroon et al., 1991; Prell et al., 1992; Quade et al., 1989, 1995; An et al., 2001). Nonetheless, we cannot completely rule out the possibility of a stronger summer monsoon for this time interval because of lower time-resolution of published records of monsoon-related indicators. It is worth noting that this time interval more or less corresponds to a time of inferred enhancement of the East Asian summer monsoon based on the relative abundance of cold-aridiphilous (CA) vs. thermo-humidiphilous (TH) mollusk assemblages in a loess-paleosol sequence on the western Chinese Loess Plateau (Li et al., 2008). The terrestrial mollusk record shows that a shift from CA to TH dominance occurred at  $\sim 5.5$ – $5.1$  Ma, corresponding to a climatic transition from a cold and dry period (7.1–5.5 Ma) dominated by 100-kyr eccentricity frequency to a warm and wet period (5.5–4 Ma) – presumably stronger summer monsoon – dominated by 41-kyr obliquity frequency (Li et al., 2008). Our  $\delta^{18}O_c$  record from the Gyirong Basin also reveals a strong eccentricity signal for the time period of 7.2–5.5 Ma, but less clear orbital signals were preserved in the 5.5–3.2-Ma interval of our record (Fig. 5), possibly due to insufficient data. The possible linkage of intensification of both Indian monsoon and East Asian summer monsoon would call for a regional (or global) rather than local cause.

In tectonically active regions such as the Himalaya, a significant change in the  $\delta^{18}O_w$  of water entering a lake basin could also be caused solely by reorganization of local or regional drainage systems feeding the lake. Such a change could be caused by a local or regional tectonic uplift in response to continuing convergence between India and Asia or a drainage capture event due to headward erosion (e.g., Brookfield, 1998), resulting in an increased mean elevation of the catchment that fed water into the lake. This interpretation is consistent with a coeval change in clay mineralogy in the Woma Formation (Fig. 4). The mineralogy of lacustrine/fluvial sediments is controlled by provenance as well as weathering regimes in the catchment area. Kaolinite is produced under high hydrolysis conditions in soils from chemical weathering of aluminum silicate minerals like feldspar (Chamley, 1989). Thus, occurrence of kaolinite in all samples examined is indicative of a much warmer and moister environment in the latest Miocene and Pliocene than today. This contrasts with Quaternary lake sediments from the Tibetan Plateau that lack kaolinite (e.g., Gasse et al., 1991; Fontes et al., 1993, 1996). An abrupt increase in the ratio of orthoclase/kaolinite at  $\sim 5.5$  Ma (Fig. 4) may suggest an increase in the strength of physical erosion, consistent with an increase in relief across the basin catchment area. This change in mineralogy is accompanied by a change in lithofacies from siltstone to sandstone (Supplementary Table 1). Unlike the  $\delta^{18}O_c$  shift that permanently changed the long-term trend of the  $\delta^{18}O_c$  record, reflecting a change in the mean environmental state of the paleo-lake basin, the sudden change in mineralogy was followed by a return to the previous state in less than 60 kyr (Fig. 4). This may be explained by a tectonic event that produced a transient increase in non-vegetated surfaces associated with freshly exposed granitic rocks in and around the Gyirong area.

This latest Miocene  $\delta^{18}\text{O}_c$  shift observed in the paleo-Woma lake basin precedes or roughly coincides (within dating uncertainty) with a major reorganization of the western Himalayan river systems (Fig. 4) documented by neodymium isotope data from drilled cores from the Arabian Sea (Clift and Blusztajn, 2005). Could the same processes that caused this major reorganization of the western Himalayan drainage systems also be responsible for this 5.5-Ma  $\delta^{18}\text{O}_c$  event seen in the paleo-Woma lake basin in the Gyirong area in the central Himalaya? The latest Miocene to Pliocene tectonic rejuvenation of the Main Central Thrust (Harrison et al., 1997; Catlos et al., 2001; Maheo et al., 2007) could have significantly altered the regional hydrological regime and drainage systems and consequently the discharge of eroded sediment to the ocean (Clift and Blusztajn, 2005). Thus, these different lines of evidence suggest that the environmental change in the paleo-Woma lake basin at  $\sim 5.5$  Ma, as indicated by a prominent negative  $\delta^{18}\text{O}_c$  shift (Fig. 4), likely reflects a major change in drainage and depositional setting possibly driven by tectonics. Additional evidence for a change in drainage system is provided by Xu et al. (this issue) showing a change in the sediment provenance and pollen assemblage at  $\sim 5.5$  Ma, which they interpret as indicating catchment extension into high elevations.

### 5.3. Paleoelevation implications

The paleoelevation of the Gyirong Basin was quantitatively determined to be  $5850 + 1410 \text{ m}/-730 \text{ m a.s.l.}$  by Rowley et al. (2001) based on the  $\delta^{18}\text{O}_w$  value of paleo-meteoric water estimated from the most negative lacustrine carbonate  $\delta^{18}\text{O}_c$  value of  $-21.5\text{‰}$  reported by Wang et al. (1996). The underlying assumptions of this paleo-elevation estimate include: (1) the carbonate was formed in the late Miocene at  $2^\circ\text{C}$ , same as today's mean annual temperature, (2) the most negative carbonate  $\delta^{18}\text{O}_c$  value records the  $\delta^{18}\text{O}_w$  of meteoric water, (3) the  $\delta^{18}\text{O}_w$  of paleo-precipitation in the late Miocene at Bakiya Khola (Nepal), which was considered as a low elevation reference site near the moisture source, was the same as the  $\delta^{18}\text{O}_w$  of soil water calculated from the  $\delta^{18}\text{O}_c$  values of paleosol carbonates and an assumed paleo-temperature, and (4) the variation in  $\delta^{18}\text{O}_w$  of meteoric water with elevation is predictable using a one-dimensional Rayleigh-type fractionation model.

Our high-resolution  $\delta^{18}\text{O}_c$  data from the Gyirong Basin (Fig. 4) show that the most negative  $\delta^{18}\text{O}_c$  values are  $-19.4\text{‰}$  for the period of 7.2–5.5 Ma and  $-22.8\text{‰}$  for  $\sim 5.5$ –3.2 Ma, which are similar to the  $\delta^{18}\text{O}_c$  value ( $-21.5\text{‰}$ ) used by Rowley et al. (2001) to reconstruct the paleo-elevation of the Gyirong Basin. However, the difference in the most negative  $\delta^{18}\text{O}_c$  values before and after 5.5 Ma is  $3.4\text{‰}$ , which would represent an increase in elevation of 1.2 km at  $\sim 5.5$ –3.2 Ma assuming that the present-day empirical  $\delta^{18}\text{O}_w$  lapse rate of  $-0.29\text{‰}/100 \text{ m}$  (Garzzone et al., 2000) applied in the past. If we were to apply the approach of Rowley et al. (2001) with the same set of assumptions to our data (Fig. 4), the paleo-elevation of the Gyirong Basin would be  $\sim 5586 + 1200/-700 \text{ m a.s.l.}$  in the late Miocene, prior to 5.5 Ma, and  $\sim 6029 + 1400/-800 \text{ m a.s.l.}$  at  $\sim 5.5$ –3.2 Ma, implying that the Gyirong Basin stood higher in the past than today and its elevation has dropped by  $\sim 2$  km since  $\sim 5.5$ –3.2 Ma. These higher-than-modern paleo-elevations inferred from the most negative  $\delta^{18}\text{O}_c$  values, although consistent with the estimate by Rowley et al. (2001), clash with the presence of significant  $\text{C}_4$  biomass (up to 100%  $\text{C}_4$ ) in the area as indicated by the carbon isotope data from fossil teeth and paleosols (Wang et al., 2006; Garzzone et al., 2000) and are also inconsistent with clay mineralogy and pollen and mammalian fossil evidence (Hsu, 1976; Ji et al., 1980; CAS, 1989; Sun et al., 2007; Xu et al., this issue).

Although precipitation is in general more depleted in  $^{18}\text{O}$  at high elevations than at low elevations, precipitation in the Himala-

yan–Tibetan region displays large  $\delta^{18}\text{O}_w$  variations on various spatial and temporal scales, which cannot be explained by elevation alone (Wang et al., 2008b). Climate factors, such as temporal changes in monsoon strength, source and history of moisture, circulation pattern and temperature, can all exert significant influences on  $\delta^{18}\text{O}$  values of meteoric water (e.g., Araguas-Araguas et al., 1998; Johnson and Ingram, 2004; Vuille et al., 2005; Wang et al., 2008b). Paleoclimate simulations using atmospheric general circulation models show that growth of mountain ranges and plateaus affects atmospheric circulation, and regional and global climate (e.g., Prell and Kutzbach, 1992; Kutzbach et al., 1993; Kitoh, 2004). Model simulations also show that changes in regional climate associated with mountain/plateau uplift have a large influence on the  $\delta^{18}\text{O}_w$  of precipitation as well as the  $\delta^{18}\text{O}_w$  lapse rate (Ehler and Poulsen, 2009; Poulsen et al., 2010). An elevation estimate of an area during a geologic period using an empirical  $\delta^{18}\text{O}_w$  vs. elevation relationship or a Rayleigh-type fractionation model would be reliable only if the climate conditions of the study area during the geologic time of interest were the same as that of today. This assumption is clearly invalid for the Gyirong area where various lines of evidence indicate a warm and humid climate in the late Miocene (Hsu, 1976; Ji et al., 1980; CAS, 1989; Wang et al., 2006; Sun et al., 2007), very different from today's cold and dry environment.

Another quantitative paleoaltimetry approach uses estimates of paleo-temperatures and temperature–elevation relationships (e.g., Quade et al., 2007; Wang et al., 2008a). By applying a new fossil-based paleo-thermometer (Zanazzi et al., 2007) to the  $\delta^{18}\text{O}$  values of fossil bone carbonate and tooth enamel, we estimated the elevation of the paleo-Woma Lake basin to be about  $2 \pm 1 \text{ km a.s.l.}$  at  $\sim 7$  Ma (see Section 4.3), which is compatible with fossil mammalian and pollen assemblages (Ji et al., 1980; CAS, 1989; Sun et al., 2007; Xu et al., this issue), carbon isotope data (Wang et al., 2006) and sediment clay mineralogy. However, a lower paleo-Woma lake basin does not exclude the possibility that there could have been both high and low elevations around the paleo-lake basin.

Limited water isotope data from southern Tibet suggest that the present-day precipitation at  $\sim 2$  km elevation – equivalent to the estimated elevation of the paleo-Woma lake basin – should have an average  $\delta^{18}\text{O}_w$  value of  $\sim -12\text{‰}$  (Garzzone et al., 2000), which is 6–7‰ higher than the estimated  $\delta^{18}\text{O}_w$  in the paleo-Woma lake basin at  $\sim 7$  Ma (see Section 4.3). The “unexpectedly” low  $\delta^{18}\text{O}_w$  in the latest Miocene in the area can be explained by the “amount effect” (Dansgaard, 1964). Although precipitation isotopic studies in the Himalaya and Tibetan region are relatively few and of short duration, data available from the IAEA-GNIP (International Atomic Energy Agency Global Network for Isotopes in Precipitation) database (IAEA, 2010) show that precipitation  $\delta^{18}\text{O}_w$  values at a given site in the Asian monsoon region display large seasonal variations and are primarily controlled by the “amount effect” (Johnson and Ingram, 2004; Wang et al., 2008b). In Lhasa ( $29.42^\circ\text{N}$ ,  $91.08^\circ\text{E}$ ,  $3649 \text{ m a.s.l.}$ ), which is the only IAEA-GNIP station in Tibet, weighted mean monthly average precipitation  $\delta^{18}\text{O}_w$  values (for the period of 1986–1992) varied from  $-6.2\text{‰}$  to  $-22.06\text{‰}$  and are strongly negatively correlated with the precipitation amounts with an amount effect of  $-9.54\text{‰}/100 \text{ mm}$  ( $r = -0.84951$ ). That is, a 100 mm increase in summer precipitation amount, equivalent to about 25% increase in annual precipitation in the area, would reduce the present-day  $\delta^{18}\text{O}_w$  value by 9.5‰. In Kunming ( $25.01^\circ\text{N}$ ,  $102.41^\circ\text{E}$ ,  $1892 \text{ m a. s. l.}$ ), which is another IAEA-GNIP station in southwest China, the available data (1986–2001) show an amount effect of  $-3.7\text{‰}/100 \text{ mm}$  ( $r = -0.78173$ ), suggesting that a 200 mm increase in summer precipitation amount could lead to a reduction in the present-day  $\delta^{18}\text{O}_w$  by 7.4‰. The present-day annual precipitation in the Gyirong area is less than 380 mm. Although the mag-

nitudes of the amount effect in both the Gyirong Basin and the paleo-Woma lake basin are unknown, the above analyses of available data from Lhasa and Kunming suggest that an increase in the amount of rainfall by 100–200 mm or more could conceivably lower the  $\delta^{18}\text{O}_w$  value by  $>7\%$ . Thus, the “unexpectedly” low  $\delta^{18}\text{O}_w$  value at  $\sim 7$  Ma estimated from fossil enamel  $\delta^{18}\text{O}$  data can be explained by higher amounts of precipitation in the paleo-Woma lake basin at that time, which is consistent with a much wetter climate in the latest Miocene (than today) as inferred from various lines of evidence discussed above (i.e., fossil assemblages, clay mineralogy, carbon isotopes).

#### 5.4. Tectonic implications

As discussed in the previous sections, our isotopic data, in conjunction with sedimentology of the Woma Formation, suggest major changes in depositional and hydrologic conditions at  $\sim 7.2$  Ma,  $\sim 5.5$  Ma and  $\sim 3.2$  Ma (Fig. 4). The 7.2-Ma event was the start of lacustrine deposition in the region. Based on the presence of significant  $\text{C}_4$  biomass (up to 100%  $\text{C}_4$ ) in the Gyirong-Thakkhola area as evidenced by carbon isotope data from fossil enamels and paleo-

sols, the inferred habitats for the fossil mammalian fauna, pollen assemblages preserved in lacustrine sediments, sediment clay mineralogy, and paleo-temperature estimates, we suggest that the initial deposition of the Woma Formation must have occurred under a much warmer and wetter climatic condition and at an elevation of  $\sim 2$  km, which is about 2–2.5 km below the current elevation of the Gyirong Basin where the studied strata are exposed. Our data also indicate a prominent negative  $\delta^{18}\text{O}$  shift and a sudden and transient change in mineralogy of sediments at  $\sim 5.5$  Ma, which may be related to reorganization of the drainage system feeding surface water into the paleo-Woma lake. This inference of drainage change is also supported by the provenance and pollen data reported by Xu et al. (this issue). The 3.2-Ma event was expressed by a change in depositional environment from a lacustrine setting to an alluvial setting. The sudden influx of proximal alluvial-fan sediments suggests a rapid establishment of local topographic relief. Here, we place the above events in the context of regional tectonic development of the central Himalaya (Fig. 1).

It is well known that tectonic uplift of the central Himalaya started at  $\sim 20$  Ma or earlier related to the development of the Main Central Thrust (MCT) system to the south (e.g., Hubbard and Har-

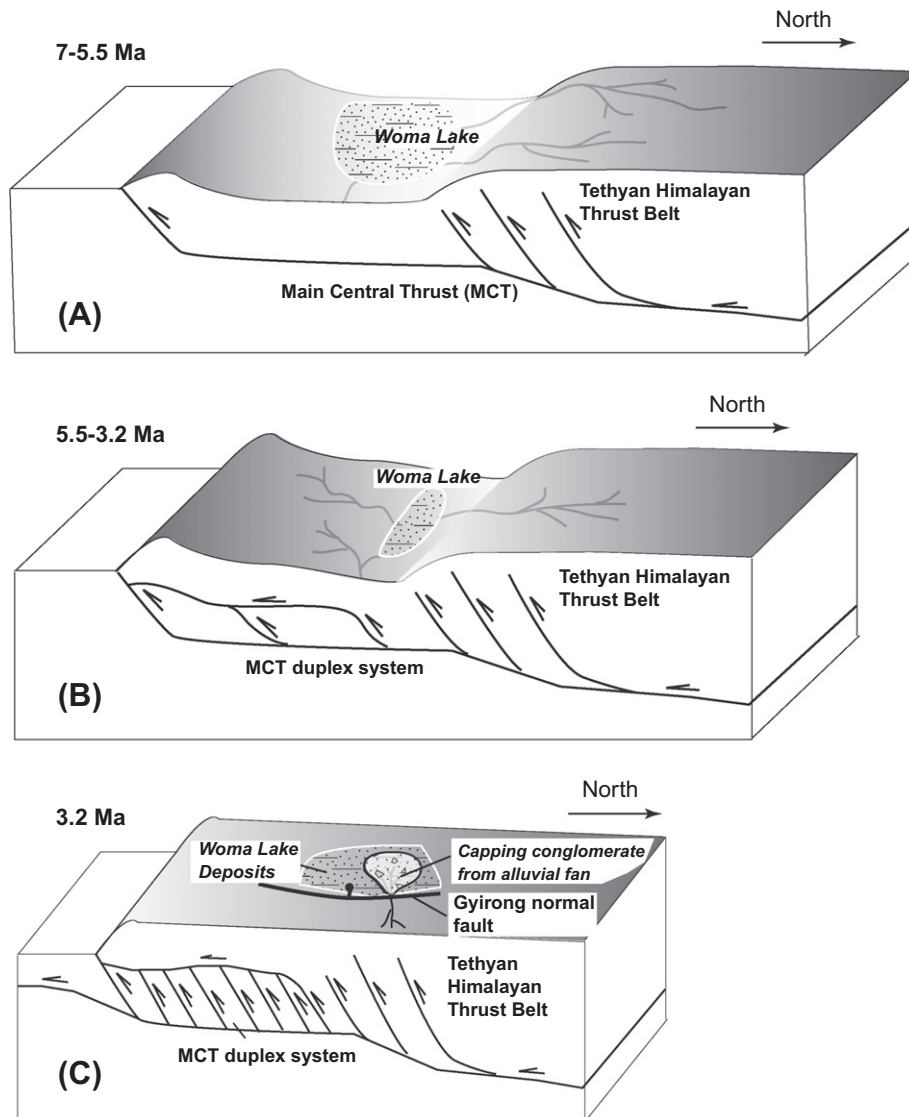


**Fig. 7.** A piggyback basin model for the evolution of the Gyirong area in the central Himalaya. (A) Miocene development of the Main Central Thrust produced a piggyback basin in its hanging wall south of the Tethyan Himalayan thrust belt at  $\sim 7.2$  Ma. (B) By  $\sim 5.5$  Ma, out-of-sequence development of the MCT duplex system uplifted part of the piggyback basin and changed the drainage configuration that fed surface water into the paleo-Woma lake. (C) At  $\sim 3.2$  Ma, the rapid development of the Gyirong rift produced large topographic relief, resulting in the deposition of conglomerate over the Woma lacustrine deposits.

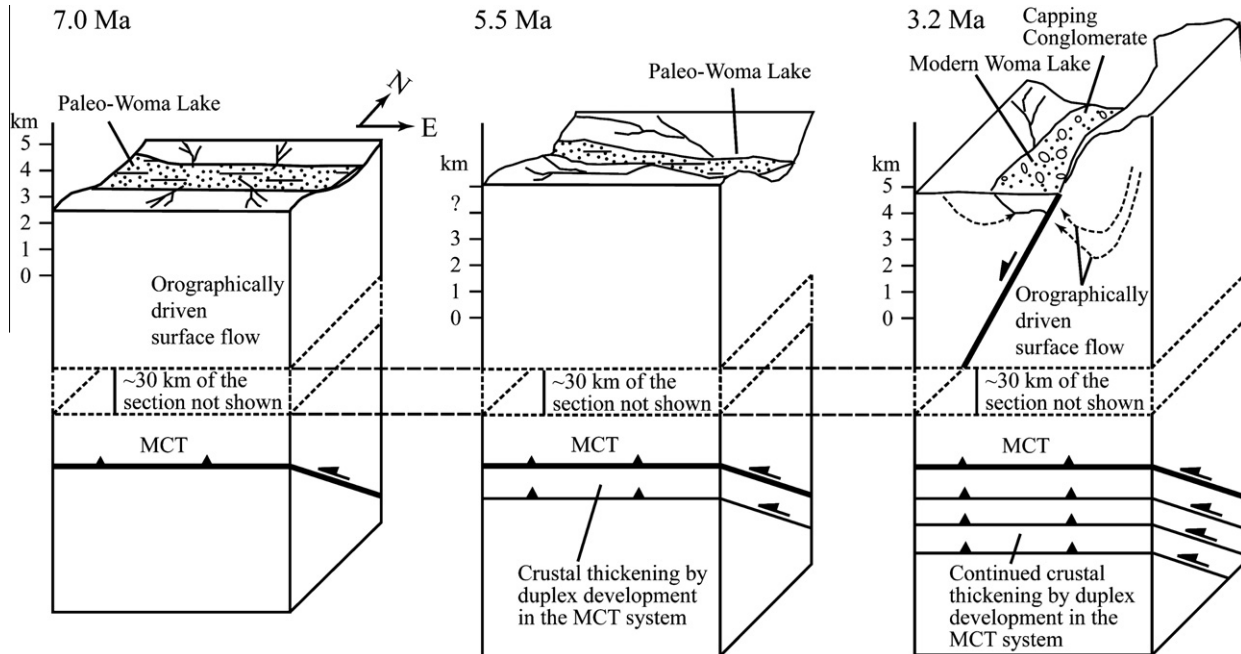


**Fig. 8.** A rift basin model for the evolution of the Gyirong area. (A) Initiation and early development of the Gyirong normal fault lowered the elevation of its related rift basin to an elevation at 2 km (not shown). At  $\sim 7.2$  Ma, the rifting process produced a topographic depression that began to accumulate lacustrine deposits. (B) At  $\sim 5.5$  Ma, rifting further deepened the basin, producing fining upward sedimentation at a slower average sedimentation rate. Drainage systems feeding surface waters into the lake also experienced a major reorganization, possibly induced by lateral propagation of the rift system. (C) At  $\sim 3.2$  Ma, lacustrine sedimentation was replaced by alluvial fan deposition, possibly induced by a rapid increase in topographic relief across the rift zone or by drainage system reorganization that rapidly drained the paleo-Woma lake.

risson, 1989; Hodges et al., 1996; DeCelles et al., 2001; Kohn et al., 2005) and the Tethyan Himalayan thrust belt to the north (see review by Yin and Harrison (2000) and Yin (2006)). Motion on the hanging wall of the MCT (where our study area is located) could have raised the elevation of the area since at least 20 Ma if the study area has been translated over a thrust ramp. Our study area also lies on the southern edge of the Tethyan Himalayan thrust belt, which was developed in the Paleogene and had accommodated >50% crustal shortening (Ratschbacher et al., 1994). The MCT was reactivated at 7–3 Ma possibly related to the development of a new thrust duplex system in the interior of the central Himalaya (Harrison et al., 1997; Catlos et al., 2001; Robinson et al., 2003). Given such overwhelming geologic evidence for early contraction and uplift of the central Himalaya, it is puzzling that the Gyirong area was located at only about 2 km at 7 Ma. There are two possible interpretations.

First, the paleo-Woma lake was developed as a piggyback basin at  $\sim 7.2$  Ma in the hanging wall of the MCT south of the Tethyan Himalayan thrust belt (Fig. 7a). Its paleogeographic setting may have been similar to the modern Kashmir Basin at the western end of the Himalayan orogen (Fig. 1), which has an average elevation of about 2 km with externally drained lakes, but is surrounded by high mountains with elevations exceeding 5 km both to south and north (Fig. 7a). The piggyback basin had stayed at an elevation of  $\sim 2$  km until the MCT system was rejuvenated at  $\sim 5.5$  Ma, causing crustal thickening below the paleo-Woma lake (Fig. 7b). This event may have also caused reorganization of the drainage systems around the paleo-Woma lake as indicated by a rapid change in  $\delta^{18}\text{O}$  value at this time in its sediments. At  $\sim 3.2$  Ma, the Gyirong rift was fully developed, which produced a through-going south-flowing river that drained and emptied the paleo-Woma lake. Meanwhile, rifting induced rapid deposition of coarse-grained sediments shed from the uplifted rift shoulders (Fig. 7c). This model predicts the former extent of the Woma Formation to be much greater than its current occurrence in the Gyirong basin and the greater extent would be along the strike direction of the MCT.

Alternatively, the deposition of the Woma Formation would represent the initiation of the Gyirong rift, with the changes in isotopic signatures and the depositional setting of the paleo-Woma lake related to different developmental stages of a single rift (Fig. 8). This model requires the Woma Formation to be restricted to the Gyirong Basin (Fig. 8). It would also require the Gyirong region to have had a higher altitude than 2 km before the start of the deposition of the conglomeratic Danzengzhukang Formation beneath the Woma Formation (Xu et al., *this issue*) with subsequent rifting lowering the elevation of the rift-valley floor. However, no sediments were stored in the rift valley until  $\sim 7.2$ –10 Ma when a sluggish drainage system developed as expressed by the formation of an externally-drained lake (Fig. 8a). Extension then caused the rift basin and the associated lake to deepen. Meanwhile, the rift basin, together with the lake and its catchment, was uplifted to a high elevation due to crustal shortening below (Fig. 8b). Finally, rapid uplift associated with rifting created higher topographic relief with large alluvial fans developed across the rift basin (Fig. 8c).

## 6. Conclusions

Oxygen and carbon isotopic analyses of the latest Miocene–Pliocene lacustrine-fluvial Woma Formation from the central Himalaya reveal an alternating wetter and drier climate pattern. Preliminary spectral analyses show periodicities of 24 and 100 kyr between 7.2 Ma and 5.5 Ma and possibly extending to 3.2 Ma, suggesting orbital forcing. Our isotope data, together with existing sedimentologic data, also reveal three major hydrological events in the late Miocene and Pliocene. The first major event was the initiation of a paleo-lake system at  $\sim 7.2$  Ma. The study area was under a much warmer and wetter climate at an elevation of  $\sim 2$  km at  $\sim 7$  Ma. The second major event happened at  $\sim 5.5$  Ma, as indicated by a significant shift to overall more negative  $\delta^{18}\text{O}_c$  values and a sudden and transient change in mineralogy of sediments, likely reflecting a major reorganization of the drainage sys-

tem that led to catchment with a larger proportion of surface water sources at higher elevations than prior to 5.5 Ma. The third major event was expressed by a change in depositional environment from a lake basin setting to an alluvial setting at ~3.2 Ma, suggesting a rapid establishment of local topographic relief. Two tectonic models may explain the above observations. The first is that the Woma Formation was deposited in a piggyback basin on the hanging wall of the Main Central Thrust. Later crustal thickening related to out-of-sequence thrusting of the MCT system raised its elevation to the current altitude. Alternatively, the Woma Formation was deposited in a rift valley and was at a low elevation at the time of its deposition. The rift basin was subsequently raised by crustal shortening from below in the interior of the Himalaya. Differentiating the two models requires more detailed work on the spatial extent, sedimentology, and structural origin of the Woma Formation.

## Acknowledgements

We thank Dr. S. Nielsen for discussions about data analysis. We are grateful to Drs. David Fox, Guillaume Dupont-Nivet and Joe Saylor for their thoughtful comments and helpful suggestions that greatly contributed to the improvement of this manuscript. This study was supported by Grants from the US National Science Foundation through its Sedimentary Geology and Paleobiology and Instrumentation and Facilities programs (EAR 0716235, EAR-0517806), Chinese Academy of Sciences (KZCX2-YW-Q09 and -120) and National Natural Science Foundation of China (NSFC 40730210).

## Appendix A. Supplementary material

Supplementary data associated with this article can be found, in the online version, at [doi:10.1016/j.jseaes.2011.05.020](https://doi.org/10.1016/j.jseaes.2011.05.020).

## References

- An, Z., Kutzback, J., Prell, W., Porter, S., 2001. Evolution of Asian monsoons and phased uplift of the Himalaya-Tibetan plateau since Late Miocene times. *Nature* 411, 62–66.
- Araguas-Araguas, L., Froehlich, K., Rozanski, K., 1998. Stable isotope composition of precipitation over southeast Asia. *Journal of Geophysical Research* 103, 28721–28742.
- Barry, J., Flynn, L., 1990. Key biostratigraphic events in the Siwalik sequence. In: Lindsay, E.H., Fahlbusch, V., Mein, P. (Eds.), *European Neogene Mammal Chronology*. Plenum Press, New York, pp. 557–571.
- Barry, J., Morgan, M., Flynn, L., Pilbeam, D., Behrensmeyer, A., Raza, S., Khan, I., Badgley, C., Hicks, J., Kelley, J., 2002. Faunal and environmental change in the late miocene Siwaliks of Northern Pakistan. *Paleobiology Memoir* 3 (28), 1–71.
- Blisniuk, P., Hacker, B., Glodny, J., Ratschbacher, L., McWilliams, M., Calvert, A., 2001. Normal faulting in central Tibet since at least 13.5 Myr ago. *Nature* 412, 628–632.
- Boutton, T., Harrison, A., Smith, B., 1980. Distribution of biomass of species differing in photosynthetic pathway along an altitudinal transect in southeastern Wyoming grassland. *Oecologia* 45, 287–298.
- Bradley, R., Keimig, F., Diaz, H., 2004. Projected temperature changes along the American cordillera and the planned GCOS network. *Geophysical Research Letters* 31, L16210.
- Bradley, R., Vuille, M., Diaz, H., Vergara, W., 2006. Threats to water supplies in the tropical Andes. *Science* 312, 1755–1756.
- Brookfield, M.E., 1998. The evolution of the great river systems of southern Asia during the Cenozoic India-Asia collision: rivers draining southwards. *Geomorphology* 22, 285–312.
- Burkle, L., 1989. Distribution of diatoms in the northern Indian Ocean: relationship to physical oceanography. *Marine Micropaleontology* 15, 53–65.
- CAS: Tibetan expedition team members, 1989. *Palaentology of Tibet - The Comprehensive Scientific Expedition to the Qinghai-Xizang Plateau, Book 1*. Chinese Academy of Sciences, Science press, Beijing.
- Catlos, E., Harrison, T., Kohn, M., Grove, M., Ryerson, F., Manning, C., Upreti, B., 2001. Geochronologic and thermobarometric constraints on the evolution of the Main Central Thrust, central Nepal Himalaya. *Journal of Geophysical Research* 106, 16177–16204.
- Chamley, H., 1989. *Clay Sedimentology*. Springer-Verlag, Berlin.
- Cina, S., Yin, A., Grove, M., Dubey, C., Shukla, D., Kelty, T., Gehrels, G., Foster, D., 2009. Gangdese Arc detritus within the eastern Himalayan Neogene foreland basin: implications for the Neogene evolution of the Yalu-Brahmaputra river system. *Earth and Planetary Science Letters* 285, 150–162.
- Clift, P., Blusztajn, J., 2005. Reorganization of the western Himalayan rivers system after five million years ago. *Nature* 438, 1001–1003.
- Dansgaard, W., 1964. Stable isotopes in precipitation. *Tellus* 16, 436–468.
- DeCelles, P.G., Robinson, D.M., Quade, J., Ojha, T.P., Garzzone, C.N., Copeland, P., Upreti, B.N., 2001. Stratigraphy, structure, and tectonic evolution of the Himalayan fold-thrust belt in western Nepal. *Tectonics* 20, 487–509.
- DeCelles, P., Quade, J., Kapp, P., Fan, M., Dettman, D., Ding, L., 2007. High and dry in central Tibet during the Late Oligocene. *Earth and Planetary Science Letters* 253, 389–401.
- Dettman, D., Fang, X., Garzzone, C., Li, J., 2003. Uplift-driven climate change at 12 Ma: a long  $\delta^{18}O$  record from the NE margin of the Tibetan plateau. *Earth and Planetary Science Letters* 214, 267–277.
- Dupont-Nivet, G., Krijgsman, W., Langereis, C.G., Abels, Hemmo A., Dai, Shuang, Fang, Xiaomin, 2007. Tibetan plateau aridification linked to global cooling at the Eocene-Oligocene transition. *Nature* 445, 635–638.
- Edwards, E., Osborne, C., Stromberg, C., Smith, S., et al., 2010. The origin of C4 grasslands: integrating evolutionary and ecosystem science. *Science* 328, 587–591.
- Ehler, T., Poulsen, C., 2009. Influence of Andean uplift on climate and paleoaltimetry estimates. *Earth and Planetary Science Letters* 281, 238–248.
- Fontes, J., Melieres, F., Gibert, E., Liu, Q., Gasse, F., 1993. Stable isotope and radiocarbon balances of two Tibetan lakes (Sumxi Co, Longmu Co) from 13,000 BP. *Quaternary Science Reviews* 12, 875–887.
- Fontes, J., Gasse, F., Gibert, E., 1996. Holocene environmental changes in Lake Bangong basin (Western Tibet) – part 1: chronology and stable isotopes of carbonates of a Holocene lacustrine core. *Palaeogeography, Palaeoclimatology, Palaeoecology* 120, 25–47.
- Garzzone, C., Dettman, D., Quade, J., DeCelles, P., Butler, R., 2000. High times on the Tibetan Plateau: paleoelevation of the Thakkhola graben, Nepal. *Geology* 28, 339–342.
- Gasse, F., Arnold, M., Fontes, J., Fort, M., Gibert, E., Huc, A., Li, B., Li, Y., Liu, Q., Melieres, F., Van Campo, E., Wang, F., Zhang, Q., 1991. A 13,000-year climate record from western Tibet. *Nature* 353, 742–745.
- Gonfiantini, R., 1986. Environmental isotopes in lake studies. In: Fritz, P., Fontes, J.-Ch. (Eds.), *Handbook of Environmental Isotope Geochemistry: The Terrestrial Environment*, vol. 2. Elsevier, Amsterdam, The Netherlands, pp. 113–168.
- Guiot, J., Goeury, C., 1996. PPPBase, a software for statistical analysis of paleoecological and paleoclimatological data. *Dendrochronologia* 14, 295–300.
- Harrison, T.M., Copeland, P., Kidd, W.S.F., Yin, A., 1992. Raising Tibet. *Science* 255, 1663–1670.
- Harrison, M., Copeland, P., Kidd, W., Lovera, O., 1995. Activation of the Nyaingtanghla shear zone: implications for uplift of the southern Tibetan Plateau. *Tectonics* 14, 658–676.
- Harrison, T., Ryerson, F., Fort, P., Yin, A., Lovera, O., Catlos, E., 1997. A late Miocene-Pliocene origin for the central Himalayan inverted metamorphism. *Earth and Planetary Science Letters* 146, E1–E7.
- Hodell, D., Curtis, J., Jones, G., Higuera-Gundy, A., Brenner, M., Binford, M., Dorsey, K., 1991. Reconstruction of Caribbean climate change over the past 10,500 years. *Nature* 352, 790–793.
- Hodges, K.V., Parrish, R.R., Searle, M.P., 1996. Tectonic evolution of the central Annapurna Range, Nepalese Himalayas. *Tectonics* 15, 1264–1291.
- Hofstra, J., Aksornkoae, S., Atmowidjojo, S., Banaag, J., Santosa, R., Sastrohoetomo, A., Thu, L., 1972. A study on the occurrence of plants with a low CO<sub>2</sub> compensation point in different habitats in the tropics. *Annales Bogorien* 5, 143–157.
- Horton, B., Dupont-Nivet, G., Zhou, J., Waanders, G., Butler, R., Wang, J., 2004. Mesozoic-Cenozoic evolution of the Xining-Minhe and Dangchang basins, northeastern Tibetan Plateau: magnetostratigraphic and biostratigraphic results. *Journal of Geophysical Research - Solid Earth* 109, B044.
- Hsu, J., 1976. On the palaeobotanical evidence for continental drift and Himalayan uplift. *Palaeobotanist* 25, 131–142.
- Hubbard, M.S., Harrison, T.M., 1989.  $^{40}Ar/^{39}Ar$  age constraints on deformation and metamorphism in the MCT Zone and Tibetan Slab, eastern Nepal Himalaya. *Tectonics* 8, 865–880.
- IAEA, 2010. <<http://nucleus.iaea.org/CIR/CIR/GNIP/HTML>>.
- Ji, H., Hsu, C., Huang, W., 1980. In: Qinghai-Tibetan Plateau Comprehensive Scientific Investigation Team of Chinese Academy of Sciences (Ed.), *Paleontology of Tibet, Qinghai-Tibetan Plateau Scientific Investigation Series, Part 1*. Science Press, Beijing, pp. 18–32.
- Johnson, K., Ingram, B., 2004. Spatial and temporal variability in the stable isotope systematics of modern precipitation in China: implications for paleoclimate reconstructions. *Earth and Planetary Science Letters* 220, 365–377.
- Jolivet, M., Brunel, M., Seward, D., Xu, Z., Yang, J., Malavieille, J., Roger, F., Leloup, A., Arnaud, N., Wu, C., 2003. Neogene extension and volcanism in the Kunlun fault zone, northern Tibet: New constraints on the age of the Kunlun fault. *Tectonics* 22, 1052. doi:10.1029/2002TC001428.
- Kim, S., O'Neil, J., 1997. Equilibrium and nonequilibrium oxygen isotope effects in synthetic carbonates. *Geochimica et Cosmochimica Acta* 61, 3461–3475.
- Kitoh, A., 2004. Effects of mountain uplift on East Asian summer climate investigated by a coupled atmosphere-ocean GCM. *Journal of Climate* 17, 783–802.
- Kohn, M., Cerling, T.E., 2002. Stable isotope compositions of biological apatite. In: Kohn, M., Rakovan, J., Hughes, J. (Eds.), *Phosphates-Geochemical, Geobiological,*

- and Materials Importance, Reviews in Mineralogy & Geochemistry, vol. 48. Mineralogical Society of America, Washington D.C., pp. 455–488.
- Kohn, M., Law, J., 2006. Stable isotope chemistry of fossil bone as a new paleoclimate indicator. *Geochimica et Cosmochimica Acta* 70, 931–946.
- Kohn, M.J., Wieland, M.S., Parkinson, C.D., Upreti, B.N., 2005. Five generations of monazite in Langtang gneisses: implications for chronology of the Himalayan metamorphic core. *Journal of Metamorphic Geology* 23 (5), 399–406.
- Kroon, D., Steens, T., Troelstra, S., 1991. Onset of monsoonal related upwelling in the western Arabian Sea as revealed by planktonic foraminifers. In: *Prell, W. et al. (Eds.), Proceedings of the Ocean Drilling Program, Scientific Results*, vol. 117. Ocean Drilling Program, College Station, Texas, pp. 257–263.
- Kutzbach, J., Guetter, P., Ruddiman, W., Prell, W., 1989. Sensitivity of climate to late Cenozoic uplift in southern Asia and the American west: numerical experiments. *Journal of Geophysical Research* 94, 18393–18407.
- Kutzbach, J., Prell, W., Ruddiman, W., 1993. Sensitivity of Eurasian climate to surface uplift of the Tibetan Plateau. *The Journal of Geology* 101, 177–190.
- Lacassin, R., Valli, F., Arnaud, N., Leloup, P.H., Paquette, J.L., Haibing, L., Tapponnier, P., Chevalier, M.L., Guillot, S., Maheo, G., Xu, Z.Q., 2004. Large-scale geometry, offset and kinematic evolution of the Karakorum fault. *Tibet: Earth and Planetary Science Letters* 219, 255–269.
- Learn, C., Elderfield, H., Wilson, P., 2000. Cenozoic deep-sea temperatures and global ice volumes from Mg/Ca in benthic foraminiferal calcite. *Science* 287, 269–272.
- Levi, N., Cerling, T.E., Passey, B., Harris, J., Ehleringer, J., 2006. A stable isotope aridity index for terrestrial environments. *PNAS* 103, 11201–11205.
- Li, F., Rousseau, D., Wu, N., Hao, Q., Pei, Y., 2008. Late Neogene evolution of the East Asian monsoon revealed by terrestrial mollusk record in Western Chinese Loess Plateau: from winter to summer dominated sub-regime. *Earth and Planetary Science Letters* 274, 439–447.
- Li, J.Z., Wang, G.A., Liu, X.Z., Han, J.M., Liu, M., Liu, X.J., 2009. Variations in carbon isotope ratios of C3 plants and distribution of C4 plants along an altitudinal transection the eastern slope of Mount Gongga. *Science in China Series D: Earth Sciences* 52 (11), 1714–1723. doi:10.1007/s11430-009-0170-4.
- Liu, T.S., Ding, M.G., Derbyshire, E., 1996. Gravel deposits on the margins of the Qinghai-Xizang Plateau, and their environmental significance. *Palaeogeography, Palaeoclimatology, Palaeoecology* 120, 159–170.
- Lu, H., Wu, N., Gu, Z., Guo, Z., Wang, L., Wu, H., Wang, G., Zhou, L., Han, J., Liu, T., 2004. Distribution of carbon isotope composition of modern soils in the Qinghai-Tibetan Plateau. *Biogeochemistry* 70, 273–297.
- Maheo, G., Leloup, P., Valli, F., Lacassin, R., Arnaud, N., Paquette, J., Fernandez, A., Haibing, L., Farley, K., Tapponnier, P., 2007. Post 4 Ma initiation of normal faulting in southern Tibet: constraints from the Kung Co half graben. *Earth and Planetary Science Letters* 256, 233–243.
- Manabe, S., Broccoli, A., 1990. Mountains and arid climates of middle latitudes. *Science* 247, 192–194.
- Maslin, M., Li, X.S., Loutre, M.F., Berger, A., 1998. The contribution of orbital forcing to the progressive intensification of northern hemisphere glaciation. *Quaternary Science Review* 17, 411–426.
- Molnar, P., 2005. Mio-Pliocene growth of the Tibetan Plateau and evolution of east Asian climate. *Palaeontologia Electronica* 8, 1–23.
- Molnar, P., England, P., Martinod, J., 1993. Mantle dynamics, uplift of the Tibetan Plateau, and the Indian monsoon. *Reviews of Geophysics* 31, 357–396.
- Murphy, M., Yin, A., Kapp, P., Harrison, T., Manning, C., Ryerson, F., Ding, L., Guo, J., 2002. Structural evolution of the Gurla Mandhata detachment system, southwest Tibet: implications for the eastward extent of the Karakoram fault system. *Geological Society of America Bulletin* 114, 428–447.
- Murphy, M., Saylor, J., Ding, L., 2009. Late Miocene topographic inversion in southwest Tibet based on integrated paleoelevation reconstructions and structural history. *Earth and Planetary Science Letters* 282, 1–9.
- Passey, B., Cerling, T., Levin, N., 2007. Temperature dependence of oxygen isotope acid fractionation for modern and fossil tooth enamels. *Rapid Communications in Mass Spectrometry* 2853, 2859.
- Poulsen, C., Ehlers, T., Insel, N., 2010. Onset of convective rainfall during gradual late Miocene rise of the Central Andes. *Science* 328, 490–493.
- Prell, W., Kutzbach, J., 1992. Sensitivity of the Indian monsoon to forcing parameters and implications for its evolution. *Nature* 360, 647–652.
- Prell, W., Murray, D., Clemens, S., Anderson, D., 1992. Evolution and variability of the Indian Ocean summer monsoon: Evidence from the western Arabian Sea drilling program. In: *Duncan, R. et al. (Eds.), Synthesis of Results from Scientific Drilling in the Indian Ocean, Geophys. Monogr. Ser.*, vol. 70. AGU, Washington, D. C., pp. 447–469.
- Quade, J., Cerling, T., Bowman, J., 1989. Development of Asian monsoon revealed by marked ecological shift during latest Miocene in northern Pakistan. *Nature* 342, 163–166.
- Quade, J., Cerling, T.E., Barry, J.C., Morgan, M.E., Pilbeam, D.R., Chivas, A.R., Lee-Thorp, J.A., ver der Merwe, N.J., 1992. A 16-Ma record of paleodiet using carbon and oxygen isotopes in fossil teeth from Pakistan. *Chemical Geology* 94, 183–192.
- Quade, J., Carter, J., Ojha, T., Adam, J., Harrison, T.M., 1995. Late Miocene environmental change in Nepal and the northern Indian subcontinent: stable isotopic evidence from paleosols. *Geological Society of America Bulletin* 107, 1381–1397.
- Quade, J., Garzione, C., Eiler, J., 2007. Paleoelevation reconstruction using pedogenic carbonates. *Reviews in Mineralogy & Geochemistry* 66, 53–87.
- R Development Core Team, 2009. R: A Language and Environment for Statistical Computing, version 2.9.0. R Foundation for Statistical Computing, Vienna, Austria, {ISBN} 3-900051-07-0. <http://www.R-project.org>.
- Ratschbacher, L., Frisch, W., Liu, G., Chen, C., 1994. Distributed deformation in southern and western Tibet during and after the India-Asia collision. *Journal of Geophysical Research* 99, 19,817–19,945.
- Robinson, D.M., DeCelles, P.G., Garzione, C.N., Pearson, O.N., Harrison, T.M., Catlos, E.J., 2003. Kinematic model for the Main Central thrust in Nepal. *Geology* 31, 359–362.
- Rowley, D., Currie, B., 2006. Palaeo-altimetry of the late Eocene to Miocene Lunpola Basin, central Tibet. *Nature* 439, 677–681.
- Rowley, D., Garzione, C., 2007. Stable isotope-based paleoaltimetry. *Annual Review of Earth and Planetary Sciences* 35, 463–508.
- Rowley, D., Pierrehumbert, R., Currie, B., 2001. A new approach to stable isotope-based paleoaltimetry: implications for paleoaltimetry and paleohypsometry of the High Himalaya since the late Miocene. *Earth and Planetary Science Letters* 188, 253–268.
- Rozanski, K., Araguas-Araguas, L., Gonfiantini, R., 1993. Isotopic patterns in modern global precipitation. In: *Swart, P., Lohmann, K., McKenzie, J., Savin, S. (Eds.), Climate Change in Continental Isotopic Records*. American Geophysical Union Geophysical Monograph, vol. 78. AGU, Washington, D. C., pp. 1–36.
- Saylor, J., Quade, J., Dettman, D., DeCelles, P., Kapp, P., Ding, L., 2009. The late Miocene through present paleoelevation history of southwestern Tibet. *American Journal of Science* 309, 1–42.
- Saylor, J., DeCelles, P., Quade, J., 2010. Climate-driven environmental change in the Zhada basin, southwestern Tibetan Plateau. *Geosphere* 6, 74–92.
- Shackleton, N.J., Backman, J., Zimmerman, H., Kent, D.V., Hall, M.A., Roberts, D.G., Schnitker, D., Baldauf, J.G., Desprairies, A., Homrighausen, R., Huddleston, P., Keene, J.B., Kaltenback, A.J., Krumsiek, K.A.O., Morton, A.C., Murray, J.W., Westberg-Smith, J., 1984. Oxygen isotope calibration of the onset of ice-rafting and history of glaciation in the North Atlantic region. *Nature* 307, 620–623.
- Sosdian, S., Rosenthal, Y., 2009. Deep-sea temperature and ice volume changes across the Pliocene-Pleistocene climate transition. *Science* 325, 306–310.
- Spicer, R., Harris, N., Widdowson, M., Herman, A., Guo, S., Valdes, P., Wolf, J., Kelley, S., 2003. Constant elevation of southern Tibet over the past 15 million years. *Nature* 421, 622–624.
- Sun, L.M., Yan, T.S., Tang, G.Y., Ding, X.Y., Wang, R.J., Tian, L.F., 2007. Neogene sporopollenin assemblages and paleogeography in the Gyirong basin, Tibet. *Geology in China* 34, 49–54.
- Swart, P., Burns, S., Leder, J., 1991. Fractionation of the stable isotopes of oxygen and carbon in carbon dioxide during the reaction of calcite with phosphoric acid as a function of temperature and technique. *Chemical Geology* 86, 89–96.
- Talbot, M., 1990. A review of the paleohydrological interpretation of carbon and oxygen isotopic ratios in primary lacustrine carbonates. *Chemical Geology* 80, 261–279.
- Thiede, R., Arrowsmith, J., Bookhagen, B., McWilliams, M., Sobel, E., Strecker, M., 2006. Dome formation and extension in the Tethyan Himalaya, Leo Pargil, northwest India. *Geological Society of America Bulletin* 118, 635–650.
- Tieszen, L., Senyimba, M., Imbamba, S., Troughton, J., 1979. The distribution of C3 and C4 grasses and carbon isotope discrimination along an altitudinal and moisture gradient in Kenya. *Oecologia* 37, 337–350.
- Torrence, C., Compo, G.P., 1998. A practical guide to wavelet analysis. *Bulletin of the American Meteorological Society* 79, 61–78.
- Vuille, M., Werner, M., Bradley, R., Keimig, F., 2005. Stable isotopes in precipitation in the Asian monsoon region. *Journal of Geophysical Research* 110, D23108.
- Wang, Y., Deng, T., 2005. A 25 m.y. isotopic record of paleodiet and environmental change from fossil mammals and paleosols from the NE margin of the Tibetan Plateau. *Earth and Planetary Science Letters* 236, 322–338.
- Wang, B., Li, S., Shen, X., Zhang, J., Yan, G., 1996. Formation, evolution and environmental changes of the Gyirong Basin and uplift of the Himalaya. *Science in China* 39, 401–409.
- Wang, Y., Deng, T., Biasatti, D., 2006. Ancient diets indicate significant uplift of southern Tibet after ca. 7 Ma. *Geology* 34, 309–312.
- Wang, Y., Wang, X., Xu, Y., Zhang, C., Li, Q., Tseng, Z.J., Takeuchi, G., Deng, T., 2008a. Stable isotopes in fossil mammals, fish and shells from Kunlun Pass Basin, Tibetan Plateau: paleo-climatic and paleo-elevation implications. *Earth and Planetary Science Letters* 270, 73–85.
- Wang, Y., Kromhout, E., Zhang, C., Xu, Y., Parker, W., Deng, T., Qiu, Z., 2008b. Stable isotopic variations in modern herbivore tooth enamel, plants and water on the Tibetan Plateau: implications for paleoclimate and paleoelevation reconstructions. *Palaeogeography, Palaeoclimatology, Palaeoecology* 260, 359–374.
- Wei, K., Gasse, F., 1999. Oxygen isotopes in lacustrine carbonates of West China revisited: implications for post glacial changes in summer monsoon circulation. *Quaternary Science Reviews* 18, 1315–1334.
- Xu, Y., Zhang, K., Wang, G., Jiang, S., Chen, F., Xiang, S., Dupont-Nivet, G., Hoon, C., Extended stratigraphy, palynology and depositional environments record the initiation of the Himalayan Gyirong Basin (Neogene China), *Journal of Asian Earth Sciences – special issue on Asian Climate and Tectonics* (this issue).
- Yang, X.Y., Zhang, J.J., Qi, G., Wang, D., Guo, L., Li, P.Y., 2009. Structure and deformation around the Gyirong basin, north Himalaya, and onset of the south Tibetan detachment system. *Science in China Series D–Earth Science* 52, 1046–1058.
- Yin, A., 2006. Cenozoic tectonic evolution of the Himalayan orogen as constrained by along-strike variation of structural geometry, exhumation history, and foreland sedimentation. *Earth-Science Reviews* 76, 1–131.
- Yin, A., Harrison, T.M., 2000. Geological evolution of the Himalayan-Tibetan Orogen. *Annual Review of Earth and Planetary Sciences* 28, 211–280.

- Yu, Z., Eicher, U., 1998. Abrupt climate oscillations during the last deglaciation in central North America. *Science* 282, 2235–2238.
- Yue, L., Deng, T., Zhang, R., Zhang, Z., Heller, F., Wang, J., Yang, L., 2004. Paleomagnetic chronology and record of Himalayan movements in the Longgugou section of Gyirong–Oma basin in Xizang (Tibet). *Chinese Journal of Geophysics* 47, 1135–1142.
- Zachos, J., Pagani, M.L., Sloan, L., Thomas, E., Billups, K., 2001. Trends, rhythms, and aberrations in global climate 65 Ma to present. *Science* 292, 686–693.
- Zanazzi, A., Kohn, M., MacFadden, B., Terry, D., 2007. Large temperature drop across the Eocene–Oligocene transition in central North America. *Nature* 445, 639–642.
- Zhang, P., Molnar, P., Downs, W., 2001. Increased sedimentation rates and grain sizes 2–4 Myr ago due to the influence of climate change on erosion rates. *Nature* 410, 891–897.
- Zheng, H.B., Powell, C.M., An, Z.S., Zhou, J., Dong, G.G., 2000. Pliocene uplift of the northern Tibetan Plateau. *Geology* 28, 715–718.